ΕΘΝΙΚΟ ΚΑΠΟΔΙΣΤΡΙΑΚΟ
ΠΑΝΕΠΙΣΤΗΜΙΟ ΑΘΗΝΩΝ
ΣΧΟΛΗ ΘΕΤΙΚΩΝ ΕΠΙΣΤΗΜΩΝ
ΤΜΗΜΑ ΧΗΜΕΙΑΣ

ΑΡΙΣΤΟΤΕΛΕΙΟ ΠΑΝΕΠΙΣΤΗΜΙΟ
ΘΕΣΣΑΛΟΝΙΚΗΣ
ΣΧΟΛΗ ΘΕΤΙΚΩΝ ΕΠΙΣΤΗΜΩΝ
ΤΜΗΜΑ ΧΗΜΕΙΑΣ

INTER-UNIVERSITY AND INTERDISCIPLINARY PROGRAM
OF MSc "CHEMICAL ANALYSIS - QUALITY CONTROL"

EVALUATION OF THE INTESTINAL TRANSPORT OF MAIN PHENOLIC COMPOUNDS FROM ROSEMARY EXTRACT ACROSS CACO-2 CELL MONOLAYER

THEOCHARI KONSTANTINA
CHEMIST

MSc Thesis

ATHENS, 2016

ΕΘΝΙΚΟ ΚΑΠΟΔΙΣΤΡΙΑΚΟ
ΠΑΝΕΠΙΣΤΗΜΙΟ ΑΘΗΝΩΝ
ΣΧΟΛΗ ΘΕΤΙΚΩΝ ΕΠΙΣΤΗΜΩΝ
ΤΜΗΜΑ ΧΗΜΕΙΑΣ

ΑΡΙΣΤΟΤΕΛΕΙΟ ΠΑΝΕΠΙΣΤΗΜΙΟ
ΘΕΣΣΑΛΟΝΙΚΗΣ
ΣΧΟΛΗ ΘΕΤΙΚΩΝ ΕΠΙΣΤΗΜΩΝ
ΤΜΗΜΑ ΧΗΜΕΙΑΣ

ΔΙΑΠΑΝΕΠΙΣΤΗΜΙΑΚΟ ΚΑΙ ΔΙΑΤΜΗΜΑΤΙΚΟ ΠΡΟΓΡΑΜΜΑ
ΜΕΤΑΠΤΥΧΙΑΚΩΝ ΣΠΟΥΔΩΝ
«ΧΗΜΙΚΗ ΑΝΑΛΥΣΗ - ΕΛΕΓΧΟΣ ΠΟΙΟΤΗΤΑΣ»

ΕΚΤΙΜΗΣΗ ΤΗΣ ΕΝΤΕΡΙΚΗΣ ΜΕΤΑΦΟΡΑΣ ΤΩΝ ΒΑΣΙΚΩΝ ΦΑΙΝΟΛΙΚΩΝ ΕΝΩΣΕΩΝ ΕΚΧΥΛΙΣΜΑΤΟΣ ΔΕΝΔΡΟΛΙΒΑΝΟΥ ΔΙΑΜΕΣΟΥ ΜΟΝΟΣΤΙΒΑΔΟΣ CACO-2 ΚΥΤΤΑΡΩΝ

ΘΕΟΧΑΡΗ ΚΩΝΣΤΑΝΤΙΝΑ
ΧΗΜΙΚΟΣ

ΕΡΕΥΝΗΤΙΚΗ ΕΡΓΑΣΙΑ ΔΙΠΛΩΜΑΤΟΣ ΕΙΔΙΚΕΥΣΗΣ

ΑΘΗΝΑ, 2016

EXAMINATION COMMITTEE

Associate Professor Dr. Nikolaos Thomaidis

Professor Dr. Michael Koupparis

Associate Professor Dr. Anastasios Economou

PREFACE

This MSc Thesis with title "Evaluation of the intestinal transport of main phenolic compounds from rosemary extract across Caco-2 cell monolayer" was carried out as part of completion of the Inter-university and Interdisciplinary Postgraduate Program "Chemical Analysis-Quality Control" of the Department of Chemistry at National and Kapodistrian University of Athens in the year 2016. The work has been done under supervision of the investigator Dr. Carolina Simó at Institute of Food Science Research (CIAL) within Erasmus + program at Madrid.

Several people have been crucial for the completion of this work and I'm glad to have the chance to express my gratitude to them. First of all, I would like to express my deep appreciation to Associate Professor Dr. Nikolaos Thomaidis, for his constant guidance and encouragement, without which this work would not have been possible. I would also like to thank him for his contribution in the unique opportunity to widen my perspective across Europe.

Heartfelt gratitude is due to Dr. Carolina Simó and Dr. Virginia García-Cañas, investigators of CIAL. I would like especially to thank them for sharing their vast knowledge with me and for giving me the opportunity to join their team enjoying the pleasant working environment and the excellent research facilities, which they provided me.

Special thanks go also to Carlos Alberto Cuellar Martín, Dr. Alberto Valdés Tabernero and Argyro Giannakopoulou for the support, the stimulating discussions and the beautiful moments we shared, as well as to the rest of the personnel of the laboratory of Foodomics. I have been very fortunate to be able to work with all these people in this project.

At this point I would also like to express my gratitude to the committee members Professor Dr. Michael Koupparis and Associate Professor Dr. Anastasios Economou for their true interest in this project.

Finally, I would like to acknowledge all my friends and my family for their never-ending support during these months.

ΠΕΡΙΛΗΨΗ

Το δενδρολίβανο είναι ένα γνωστό βρώσιμο βότανο, το οποίο ανήκει στην οικογένεια των χειλανθών (*Lamiaceae*) και παρουσιάζει μεταξύ άλλων αντιοξειδωτική, αντιφλεγμονώδη, αντιπολλαπλασιαστική δράση, καθώς και προφυλακτική δράση κατά του καρκίνου. Οι ευεργετικές για την υγεία ιδιότητες του δενδρολίβανου μπορούν να αποδοθούν στα φαινολικά συστατικά του, όπως το καρνοσικό οξύ (CA), την καρνοσόλη (CS), τη ροσμανόλη (RS) και το 12-O-μεθυλοκαρνοσικό οξύ (MCA). Δεδομένου ότι οι διαιτητικές φαινολικές ενώσεις μπορούν να προκαλούν βιολογικές επιδράσεις μόνο κατά την απορρόφησή τους από το έντερο, πληροφορίες για τέτοιου τύπου διεργασίες καθίστανται ζωτικής σημασίας για την εκτίμηση των πιθανών επιπτώσεών τους στην υγεία.

Αρχικά αναπτύχθηκε μια μέθοδος προσομοίωσης της γαστροεντερικής (GI) πέψης προκειμένου να εκτιμηθεί το αποτέλεσμα της GI πέψης στο προφίλ των φαινολικών ενώσεων εκχυλίσματος δενδρολίβανου (RE). Αφού πραγματοποιήθηκε χημικός χαρακτηρισμός του GI-RE, προσδιορίστηκε η κυτταροτοξική δράση του RE, καθαρού κλάσματος του GI/RE που λήφθηκε μετά από εκχύλιση στερεάς φάσης (SPE/GI-RE) και προτύπων των κύριων διτερπενίων του δενδρολίβανου σε Caco-2 κύτταρα. Ύστερα απο δοκιμές κυτταροτοξικότητας με πρότυπα, βρέθηκε ότι η RS παρουσίαζε την υψηλότερη τοξικότητα.

Στόχος της παρούσας εργασίας ήταν επίσης η μελέτη της χημικής σταθερότητας των βασικών διτερπενίων του RE. Κατά το ξεκίνημα και μετά το πέρας (6 ώρες) της επώασης, το CA, η CS, η RS και το MCA ανιχνεύθηκαν στην εσωτερική μικροκυψελίδα θαλάμου Transwell χρησιμοποιώντας μια UHPLC-TOF MS μέθοδο, κατά την παρουσία και απουσία κυττάρων. Το MCA ήταν το πιο σταθερό διτερπένιο. Αντίθετα, το CA διασπάστηκε κυρίως σε CS και RS, καθώς επίσης ανιχνεύθηκαν ροσμαδιάλη (RD) και κινόνη της ροσμανόλης (RS-Q). Το κύριο προϊόν διάσπασης της CS ήταν η RS, καθώς ανιχνεύθηκαν και η RD και η RS-Q. Τέλος, η RS διασπάστηκε σε RD και RS-Q. Κατά την παρουσία κυττάρων τα δεδομένα υπέδειξαν την πρόσληψη των φαινολικών ενώσεων από τα κύτταρα.

Η μεταφορά των CA, CS, RS και MCA μέσω του εντέρου (ως πρότυπα, σε RE και σε SPE/GI-RE) μελετήθηκε και προς τις δύο κατευθύνσεις χρησιμοποιώντας μονοστιβάδες Caco-2 κυττάρων. Οι ενώσεις προσδιορίστηκαν με UHPLC-TOF MS μέθοδο και οι παράμετροι της μεταφοράς τους υπολογίστηκαν. Οι φαινολικές ενώσεις βρέθηκε ότι

απορροφούνται πιο αποτελεσματικά με κατεύθυνση από την εξωτερική προς την εσωτερική μικροκυψελίδα. Τα αποτελέσματα αποκάλυψαν επίσης ότι τα συστατικά της μήτρας των φυτών, καθώς και η διαδικασία της εκχύλισης στερεάς φάσης μπορεί να επηρεάσει τη μεταφορά των διτερπενίων διαμέσου της μονοστιβάδος των Caco-2 κυττάρων. Οι εξεταζόμενες ενώσεις παρουσίασαν χαμηλές προς μέτριες τιμές διαπερατότητας με υψηλότερη τιμή αυτή της RS, ακολουθούμενη από την τιμή της CS, του MCA και του CA. Τέλος, σύμφωνα με τις τιμές του λόγου εκροής, ο κύριος μηχανισμός απορρόφησης των διτερπενίων μέσω του εντέρου είναι η διακυτταρική μεταφορά. Παράλληλα, η ενεργός εκροή είναι πιθανόν να συμμετάσχει στη μεταφορά του MCA.

ABSTRACT

Rosemary is a well-known edible herb from the *Lamiaceae* mint family with a variety of properties, such as, antioxidant, anti-inflammatory, chemoprotective, and antiproliferative activities. Health promoting activities may be attributed to its phenolic constituents: carnosic acid (CA), carnosol (CS), rosmanol (RS) and 12-O-Methyl carnosic acid (MCA), among others. Since dietary phenolic compounds can only produce biological effects upon intestinal absorption, information about such processes is crucial for the evaluation of their potential impact on human health.

An *in vitro* simulation of gastrointestinal (GI) digestion was developed to evaluate the effect of gastrointestinal (GI) digestion on the phenolic profile of rosemary extract (RE). After the chemical characterization of GI-RE, evaluation of cytotoxicity activity against Caco-2 cells of RE, purified fraction of GI/RE after solid phase extraction (SPE/GI-RE) and the main rosemary diterpenes took place. According to the cytotoxicity tests of the pure standards, RS exhibited the strongest toxicity.

In the aim of this work was also the study of chemical stability of the main diterpenes in the RE. At the beginning and at the ending of the incubation (6 h), CA, CS, RS and MCA were detected by UHPLC-TOF MS at the apical compartment in the presence and absence of Caco-2 cells. MCA was the more stable rosemary diterpene. On the contrary, CA was degraded mainly to CS and RS, while rosmadial (RD) and rosmanol quinone (RS-Q) were also found. The main degradation product of CS was RS. RD and RS-Q were also detected. Finally RS was degraded to RD and RS-Q. In the presence of cells the data indicated the uptake of the phenolic compounds from the cells.

The intestinal epithelial transport of CA, CS, RS and MCA (either as pure compounds or from RE and SPE/GI-RE) was investigated across Caco-2 cell monolayer in both directions. These compounds were assayed by UHPLC-TOF MS, and their transport parameters were calculated. Phenolic compounds were found to be more effectively absorbed across basolateral membrane when pure standards or diterpenes within the RE and SPE/GI-RE were studied. The data also revealed that plant matrix components and SPE procedure affect the transport of diterpenes across the Caco-2 monolayer. The tested compounds presented low to moderate permeability (P_{app}) values with RS showing the highest P_{app} value, followed by CS, MCA and then CA. Finally, efflux ratio values indicate that the main absorption mechanism of the diterpenes via intestine was transcellular transport. Active efflux transport might be involved in MCA transport.

TABLES OF CONTENTS

LIST OF ABBREVIATIONS

AP-BL	Apical to basolateral direction
BL-AP	Basolateral to apical direction
CA	Carnosic acid
Caco-2	Human intestinal cell line derived from colonic adenocarcinoma
CA-Q	Carnosic acid quinone
CS	Carnosol
DMEM	Dulbecco's modified Eagle's medium
DMSO	Dimethyl sulfoxide
EfR	Efflux ratio
EIC	Extracted ion chromatogram
GAE	mg of gallic acid per g of extract
GI	Gastrointestinal
GI-RE	Gastrointestinal digestion product from rosemary extract
HBSS	Hank's balanced salt solution
LY	Lucifer yellow
MCA	12-O-Methylcarnosic acid
MTT	3-(4,5-dimethyl-2-thiazolyl)-2,5-diphenyl-2H-tetrazolium bromide bromide
MW	Molecular weight
P_{app}	Apparent permeability coefficient, (cm/s)
P-gp	P-glycoprotein
pk_a	Negative common logarithm of acid dissociation constant
RD	Rosmadial
RE	Rosemary extract
RS	Rosmanol
RS-Q	Rosmanol quinone
RT	Retention time, (min)
SGF	Simulated gastric fluid
SIF	Simulated intestinal fluid
SPE	Solid phase extraction
SPE/GI-RE	Purified fraction of gastrointestinal digestion product of rosemary extract after solid phase extraction
TEER	Transepithelial electrical resistance
TIC	Total ion chromatogram
TPC	Total phenols content

U/GI-RE	Ultrafiltrated gastrointestinal digestion product from rosemary extract
UHPLC-TOF MS	Ultra-high performance chromatography hyphenated to time of flight mass spectrometry

CHAP.1 THEORETICAL PART

1.1. ROSEMARY AND ITS BIOACTIVE COMPOUNDS

Rosmarinus officialis, more popularly known as rosemary, is a member of the mint family *Lamiaceae*, which includes many other herbs, such as oregano, sage, thyme, basil and more others. Rosemary is a perennial evergreen shrub with needle-like leaves that grows wild in the Mediterranean basin. Nowadays, this plant is cultivated worldwide in consequence of its variants uses as a common household culinary spice for flavoring [1, 2]. Except of its use as a culinary spice to adjust flavor of food during cooking, rosemary is often used in nutraceutical area as beverage, food supplement and preservative and also in cosmetics due to the growing preference of consumers for natural products [3,4].

Rosemary leaves are known to contain a number of antioxidants compounds, thus this plant is widely employed in the food industry as a natural antioxidant for food conservation. Rosemary extract can be used as an alternative preservative in the place of synthetic antioxidants such as butylated hydroxytoluene (BHT) and butylated hydroxyanisole (BHA), which can exert carcinogenic effects in living organisms. Plant extracts having a pleasant taste and smell can dispose preventative properties, anticipating lipids deterioration, oxidation reactions and microorganism spoilage [5, 6].

During the last decades the interest for natural antioxidant products has augmented rapidly. Among the plants reported for their antioxidant activity Rosemary has been accepted as one of the species with the highest activity being the most used and commercialized between them [4]. These activities have been attributed to the presence of phenolic compounds, with carnosic acid ($C_{20}H_{28}O_4$, MW: 332.43392 g/mol), carnosol ($C_{20}H_{26}O_4$, MW: 330.41804 g/mol), rosmanol ($C_{20}H_{26}O_5$, MW: 346.41744 g/mol) and 12-Methylcarnosic acid ($C_{21}H_{30}O_4$, MW: 346.4605 g/mol) being the most important between them. Carnosic acid and carnosol are known as the principal polyphenols responsible for antioxidant and other beneficial properties of fresh rosemary leaves and rosemary extracts [7, 8]. It is reported that the dried leaves of rosemary contain approximately 2-3% carnosic acid and the other three major polyphenolic components in lesser amounts [4]. Hence, carnosic acid is the most abundant polyphenolic compound in rosemary. The composition of rosemary depends on the local environmental conditions, the season when the plant was collected, the technique used for drying, the storage conditions of the collected plants and the applied methodology for isolation of the essential oils [6]. Polyphenols are plant

secondary metabolites that contain one or more hydroxyl groups attached to a benzene ring in their chemical structure [9].

Phenolic diterpenes are composed of four isoprenes, such as carnosic acid, carnosol, rosmanol and rosmadial, triterpenes, like ursolic acid and betulinic acid, phenolic acids such as rosmarinic acid and flavonoids like genkwanin, hesperidin and cirsimartin [2, 3, 5]. Other phenolic diterpenes constitute artifacts of the principal compounds, such as 7-methoxyrosmanol and 7-methoxy-epirosmanol, which are produced when extracts containing carnosic acid or carnosol are heated in the presence of methanol or rosmaridiphenol, which is formed by the oxidation of carnosic acid. In addition, it is reported that carnosic acid turns to carnosol upon heating and that carnosol can degrade to produce other compounds, like rosmanol [4]. In general, factors such as temperature or light can induce a degradation of rosemary antioxidants into several compounds [10].

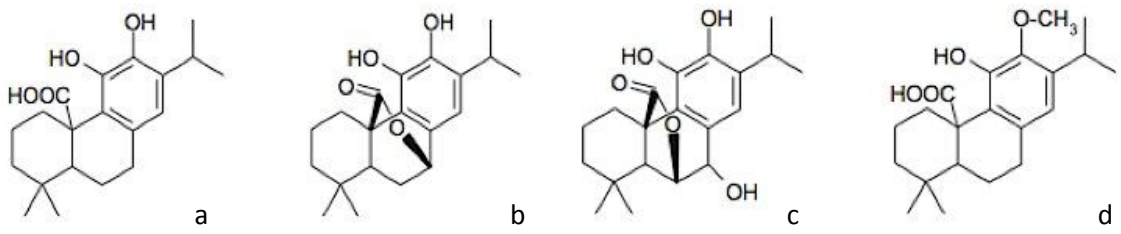

Figure 1.1. *Molecular structure of: (a) carnosic acid, (b) carnosol, (c) rosmanol and (d) 12-O-Methylcarnosic acid [11].*

Except of antioxidant activity, polyphenolic compounds attribute to rosemary much more health beneficial properties. Traditionally rosemary had a number of therapeutic applications in folk medicines in curing or managing of a wide range of diseases including treatment of common cold and gastrointestinal disturbances, respiratory disorders and inflammatory diseases. In addition, rosemary was used in the folk medicine as a healing and microbiological agent, as far as to treat diabetic patients in western Turkey [12]. Therefore, nowadays rosemary is a well-known and greatly valued medicinal herb, which is widely used in pharmaceutical products and is still examined for its further biological and pharmaceutical properties [1].

More specifically, rosemary and its polyphenolic components show antimicrobial and anti-inflammatory activities, as far as anti-tumorigenic and chemopreventive potential against different type of cancer like leukemia, prostate, colorectal, skin and breast cancer. Several polyphenols present the capacity not only to block initiation of the carcinogenic

process but also to suppress promotion and progression of cancer [3, 9, 13, 14]. In addition, rosemary can be used to prevent and treat diseases, such as ulcer, hyper-glycaemia, cardiovascular disease**,** neurological diseases like Alzheimer and metabolic diseases like diabetes, as well as to contribute to the inhibition of human immunodeficiency virus (HIV) infection and more others.

Furthermore, a number of animal studies demonstrate that rosemary extract mitigate weight gain, improve plasma glucose and lipid profiles and reduce cholesterol levels [1, 15, 16]. It is reported that biological activities of some of rosemary compounds and extracts are probably linked to their ability to reduce the oxidative damage caused by free radicals over cellular elements like DNA, proteins or membrane phospholipids by inhibiting scavenging both hydroxyl radicals and singlet oxygen. Moreover, these antioxidant molecules derived from rosemary may act as free radical scavengers but additionally might play a role by regulating the activity and/or expression of certain enzymatic systems implicated in relevant physiological processes like apoptosis, tumor promotion, intracellular signal transduction or xenobiotic-metabolizing enzymes in liver [3, 17].

1.2. PROCESS OF DIGESTION

Digestion constitutes the breaking down of food into smaller components, which can be absorbed and used by the organism or excreted [18]. The digestion in human begins at the mouth cavity. There, the food is being mechanically and chemically broken down by mastication and salivation. With mastication the food is being cut mechanically in smaller size particles. Also, the saliva contains the enzyme α-amylase. Therefore, mainly the breaking down of polysaccharides takes place in the mouth cavity [18, 19]. In that way, a mass of food known as bolus is created. After its creation, bolus is conducted to the stomach via the esophagus through peristalsis, an advancing contractile wave of the walls of a flexible conduit that forces the contents of the conduit forward. The transit of food via esophagus doesn’t have any effect on food digestion [19].

After that, the bolus reaches in the stomach, the major compartment of chemical and mechanical food digestion. The breaking down of food continues at this organ mechanically by churning provoked by the peristaltic movement of the walls of the stomach and chemically by the mixing with pepsin and some gastric lipases. There, mainly protein and peptide degradation takes places, while only 10-30% of overall triglycerides

are degraded [18]. Hydrochloric acid is also secreted into the stomach, which gradually lower the pH of the content and aid in hydrolysis [20]. The food bolus is transformed into chime, which is progressively transported to the small intestine. Liquids and small particles (< 1 to 2 mm) flow continuously from the stomach through the pyloric opening into the duodenum. Indigestible particles greater in size are squirted back into the stomach, by an action called retropulsion. This occurs repeatedly until the size of food becomes small enough [19].

In the duodenum, the low pH of the stomach is neutralized by bicarbonate. The presence of lipids stimulated the secretion of bile salts, phosphatidylocholine and cholesterol from the gall bladder, while pancreatic fluids containing digestive enzymes are secreted by pancreas. Lipases bind at the surface of oil droplets formed by the gall blander emulsifiers, the lipids are hydrolyzed into their digestion products and micelles, emulsion droplets and other colloidal species are formed. Absorption of lipophilic compounds by intestinal enterocytes will take place only if they are inside or form part of dietary mixed micelles. That's the reason why the study of digestion of lipophilic compounds is more difficult in comparison to the study of water-soluble products [18, 20].

The final stage of dietary carbohydrates and proteins digestion occurs right on the surface of small intestinal enterocytes by brush boarder enzymes, which are integral membrane proteins of enterocytes. The produced nutrients are mainly absorbed by the enterocytes of the jejunum and to a lesser extent in the ileum. After absorption by enterocytes, the compounds especially peptides can be further degraded by intracellular proteases. Subsequently, water-soluble nutrients are mainly released into the bloodstream and end up in the liver via the hepatic portal vein. Fat-soluble nutrients are incorporated into chylomicrons and transported to the lymph. After their entrance and reprocessing in the lymphatic system, these compounds also end up in the blood.

The last compartment of the gastrointestinal is the large intestine, where the absorption of water occurs. Moreover, as it is known the large intestine contains a great number of microbial population. Many of these microorganisms help in the digestion of food elements that cannot be ingested by human enzymes [20].

1.2.1. Static and dynamic *in vitro* digestion models

At the recent years many *in vitro* gastrointestinal models have been developed and widely employed in many fields of food, nutritional and medical sciences [19]. Their great success is due to their advantages in comparison to human and animal trials, which are often characterized as ethically disputable, expensive and resource intensive. Furthermore, *in vivo* methods meet limitations concerning the experimental design and great inter-individual variations. On the contrary, *in vitro* alternatives are less time-consuming, cheaper and less labor-intensive. In addition, they offer a better control of experimental variables and an easy sampling. Standardization of the conditions provides better reproducibility and also the possibility to compare the results between different research groups. However, the use of different digestion models erases this possibility due to the differences in the applied conditions between the different laboratories (e.g. differences in digestion time, variety of enzyme origin etc.) [21].

The necessity of bioavailability studies contributes to the continuous development of the digestion models, too, since there is an ever-growing need to investigate the beneficial impact of nutrients on human health and to improve food formulation and design.

The simplest techniques of digestion simulation are the static simulated gastrointestinal models, also known as biochemical models. These approaches mimic digestion by simulating the physiological conditions typical in each compartment of gastrointestinal tract, such as temperature, pH, enzymatic and chemical composition of saliva, gastric and duodenal juice and bile salts, incubation time etc. [20, 21, 22]. This type of models mimic the biochemical processes, which occur during digestion and usually use a single set of initial conditions in each compartment. They don't mimic physical processes, such as changes in conditions over time, peristalsis and others. Hence, static models are often accused for being an oversimplifying model, at which the food is simply mixed with gastric and pancreatic fluids in a shaking incubator or a water bath with integrated rotator or shaker, and that they do not represent in an accurate way the realistic conditions and parameters of digestion process [19, 21].

On the other hand, dynamic models simulate the dynamic process of digestion. They reproduce the peristaltic contraction of stomach wall and create mechanical forces comparable to those measured *in vivo*, incorporate gastric secretion and emptying and simulate the continuous change in pH. Thus, dynamic models enable an improved simulation of digestion process and prediction of transformation of food constituents into

the gastrointestinal tract [19]. However, the static models are extremely useful for the studying of simple meals and isolated or purified food components [20, 21].

Most of the static models describe a three step stimulating process, which includes oral, gastric and intestinal digestion, since these compartments (mouth, stomach and small intestine) seem to mostly determine bioaccessibility. In most of cases the large intestine tract is not taken into account, considering that the main part of food digestion and absorption takes place in the small intestine. Also, the process in mouth has duration from few seconds to minutes and the pH value is almost neutral. Therefore, no important compound dissolution from food takes place in this step. Hence, for liquid food or food components, the oral phase of digestion is often omitted [20, 21].

In any case, further comparison with data collected from *in vivo* trials in human or animals will certainly allow a better validation of the predictive capability of the *in vitro* digestion model [19].

1.2.2. Bioavailability, bioaccessibility and bioactivity

Bioavailability can be defined as the fraction of digested component, which is available for utilization in normal physiological functions. Bioavailability is determined via *in vivo* assays. It includes the digestion of the element within the gastrointestinal tract, the absorption of the element by intestinal cells and its transport into the circulation and finally the incorporation from circulation to the functional target or entity. Bioavailability involves two additional terms from which must be distinguished: bioaccessibility and bioactivity. Bioaccessibility is the fraction of a component that is released from food matrix into the gastrointestinal tract and becomes bioavailable. However, the process of absorption through epithelial tissue and the metabolism from intestine or liver are excluded from the term of bioaccessibility. On the other hand, bioactivity includes all the events related to the transportation of a nutrient or a bioactive compound to the target entity, its interaction with biomolecules and its metabolism or its biotransformation in intestine and liver, as well as the induced physiological responses [20].

1.3. *IN VITRO* INTESTINAL ABSORPTION MODEL WITH CACO-2 CELLS

1.3.1. Caco-2 cell line

One of the most used intestinal cell line is Caco-2. Caco-2 cells are originated from human colorectal carcinoma. Although they are derived from large intestine, when they are *in vitro* cultured under specific conditions they spontaneously undergo differentiation into polarized epithelial cells with some characteristics that resemble intestinal enterocytes. After reaching confluence, Caco-2 cells form differentiated monolayers and express various enterocyte digestive and hydrolyzing enzymes, as well as carrier-mediated transport systems for sugar, amino acids and several others compounds [23]. Also, differentiated Caco-2 cells form microvillus structure, a well-defined brush border on the apical surface and monolayer with tight intercellular junctions [24, 25].

Caco-2 cells have the ability to differentiate and polarize, when they are cultured on permeable filter supports [26]. Therefore, when cultured on filters separated in two compartments, they form a monolayer simulating the intestinal barrier, permitting the evaluation of absorption of a compound in humans and the investigation of transport mechanism [27]. The preparation of a fully differentiated confluent Caco-2 cell monolayer requires in general a 3-week period of cell with 9-10 change of medium [28].

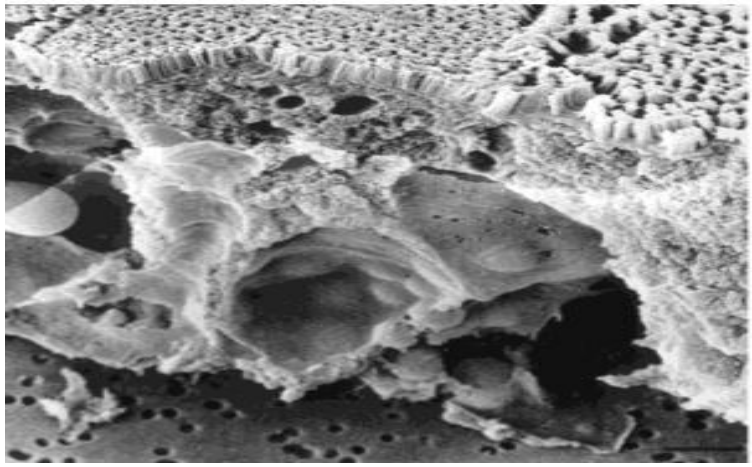

Figure 1.2. *Transmission electron microscopy of Caco-2 cells grown for 21 days to form a monolayer of enterocyte-like cells with a well-developed brush border. Adherent cells adhere through tight junctions on the apical surface of cells to form the monolayer [29].*

However, the Caco-2 monolayer model shows some differences in comparison to the small intestine tissue. The tightness of the monolayer resembles more colonic than small intestine tissue. For that reason, small hydrophilic compounds show poor permeability

through the paracellular route in comparison to *in vivo* permeability. In addition, Caco-2 layer is composed only with absorptive cells, whereas the intestinal epithelium is a conglomerate of absorptive enterocytes and other cells type such as goblet cells, endocrine cells, and M cells, with the mucus goblet cells and enterocytes representing the two most frequent phenotypes in the intestinal epithelium in the proportion of 10 and 90%, respectively [29, 30]. Regularly, a co-culture of Caco-2 and HT-29 cells is proposed as a solution, since HT-29 cells dispose goblet cells, which produce mucin. Hence, in Caco-2-HT-29 co-culture a mucus layer is formed lining the cellular Caco-2 monolayer. However, it is reported that during the use of these co-cultures as a transport model, cells of the same type tend to form a colony of pure cells, possibly altering the uniformity of the cell monolayers [31].

Another drawback of the pure Caco-2 cell system is the potential overexpression of P-glycoprotein. This overexpression can lead to higher secretion rates and lower permeability in the absorptive direction than the real one. Also, carrier-mediated absorptive transport seems to be lower in comparison to human small intestine, probably due to colonic origin of Caco-2 cell line, since carriers are expressed to a lower extent than in normal enterocytes [26, 30]. However, the permeability of drugs and other compounds correlate well with that of the small intestinal membrane *in vivo* and Caco-2 cell systems can surely be used for the prediction of oral absorption [24, 32].

1.3.2. *In vitro* absorption model

Caco-2 cell monolayers have been widely accepted as a potent *in vitro* model membrane for the rapid screening of the intestinal absorption, receiving the last decade a considerable increasing attention in many research fields including the pharmaceutical and nutrition sciences. *In vitro* Caco-2 assays for the assessment of permeability are considered faster, less laborious and less expensive in comparison to the *in vivo* assays as far as reliable. They can be used to determine the permeability of compounds through the small intestine and by extension their bioavailability and the additives that could be added to increase their absorption. Also, they can be used to investigate the mechanism of transport (active or passive) and to identify possible carriers of the compounds, and finally, to study the preliminary metabolism of compounds in the intestine [24, 30, 32].

The movement of compounds across the epithelium can occur in two directions: from apical to basolateral representing the absorptive direction from the intestinal lumen to the

underlying tissue and circulation and vice versa from basolateral to apical representing the secretory direction from the tissue out into the lumen again [33].

A compound can cross the intestinal epithelium via three pathways depending on its properties: via paracellular pathway, via transcellular pathway or through active transport.

A small hydrophilic compound displays low affinity to the lipophilic bilayer of cellular membrane, due to its hydrophilicity. Hence, it is incapable to cross transcellularly the intestinal epithelium, but it prefers the paracellular route between adjacent intestinal cells through tight junctions [26, 33].

Transcellular route is the predominant route for intestinal absorption. This pathway is followed by amphiphilic compounds, which show sufficient lipophilicity to cross the cell membrane by passive diffusion. If a compound has considerably high lipophilicity, it enters easily into the cells, though it cannot leave out of the cell and be bioavailable. Contrariwise, high lipophilic compounds often accumulate in the interior of cells [24].

Passive diffusion across intestinal epithelial cells occurs through non-specific permeability pathways and does not require any consumption of energy from the cell [33]. As the center of the lipid bilayer is highly hydrophobic, a substance diffuses down its concentration gradient across the membrane from an area of higher to an area of lower concentration [33, 34]. The rate at which a molecule diffuses across a membrane depends on its physicochemical properties such as its molecular size, the pH and its dissociation constant pk_a, its degree of hydrophobicity, the octanol-water partition coefficient and its solubility [35]. Molecules that are relatively small and lipophilic (lipid-soluble) easily enter and exit cells. On the contrary, lipid bilayers seem to be less permeable to larger molecules.

Based on permeability values the tested compounds could be grouped into three categories. Compounds with $P_{app}<2\times10^{-6}$ cm/s present low permeability, while compounds with 2×10^{-6} cm/s$<P_{app}<20\times10^{-6}$ cm/s present moderate permeability. On the other hand, $P_{app}> 20\times10^{-6}$ cm/s signifies high permeability [36].

Assessing transport in bidirectional experiments across the cell monolayer enables an efflux ratio to be determined. Efflux ratio is defined as the ratio of apparent permeability in the secretory direction to that of the absorptive direction. Possible active efflux transport can be determined on the basis of the efflux ratio. Specifically, efflux ratio values lower than 2 declare that passive transport takes place, in contrast with values higher than 2 meaning that active efflux carrier mediated transport occurs [25, 35]. Passively transported compounds should generate efflux ratios close to 1, since no active transport mechanisms

are involved and permeability from apical to basolateral should be equal to this from basolateral to apical.

Finally, it should be mentioned that although the liver is the main metabolizing organ, the gut wall could also play an important role in the first-pass metabolism of some xenobiotic compounds. The purpose of the metabolism of xenobiotics is to make them more hydrophilic and, thus they could be more easily excreted from human organism. During their intracellular transport in the small intestine, compounds may undergo Phase I and II metabolism. In Phase I the compounds are oxidized, reduced or hydrolyzed. On the contrary, in Phase II the compounds or their products from Phase I are conjugated. The conjugation reactions include sulfation, glucuronidation and -O-methylation, all of them observed during intestinal absorption according to the literature. Hence, metabolism also affects transport, since the intracellularly formed metabolites could be secreted out of the enterocytes back to the lumen of the intestine or to the circulation in a different way than their parent compounds [23, 37].

1.4. OBJECTIVE

Since dietary phenolic compounds can only produce biological effects upon gastro-intestinal digestion and intestinal absorption, information about such processes is crucial for the evaluation of their potential impact on human health. Thus, with the aim of deepening on bioaccessibility and intestinal absorption of main bioactive constituents from a rosemary extract, four objectives were established:

1. To evaluate the effect of *in vitro* gastrointestinal digestion on the phenolic profile of a rosemary extract, simulating the physiochemical and biochemical factors of the upper gastrointestinal tract.

2. *In vitro* evaluation of the cytotoxicity activity of the four rosemary diterpenes on Caco-2 cells.

3. *In vitro* study of the chemical stability of the main diterpenes in the rosemary extract.

4. *In vitro* evaluation of intestinal epithelial transport of CA, CS, RS and MCA, either as pure compounds or from a rosemary extract (digested or not) across Caco-2 cell monolayers in both apical-to-basolateral and basolateral-to-apical directions.

CHAP.2 EXPERIMENTAL PART

2.1. MATERIALS AND METHODS

2.1.1. Reagents and Materials

For the construction of the stock solutions used in gastrointestinal simulation, potassium chloride and potassium dihydrogen phosphate were purchased from Merck Millipore (Darmstadt, Germany), while sodium bicarbonate, sodium chloride and magnesium chloride hexahydrate were bought from Sigma Aldrich (USA). Ammonium carbonate was obtained from Fluka (Switzerland) and sodium hydroxide from VWR (USA). Water Purification Unit Millipore Milli Q by Merck Millipore (Darmstadt, Germany) was used for the purification of water. In addition, pepsin (from porcine gastric mucosa with enzymatic activity 3,497 units/mg protein), pancreatin from porcine pancreas (3.2 TAME UNITS/mg extract) and bile extract porcine were purchased by Sigma Aldrich. Lucifer Yellow CH dilithium, references compounds atenolol and propranolol and dimethyl sulfoxide were purchased by Sigma Aldrich, too. Methanol (LC-MaScan) was from RCI Labscan (Bangkok, Thailand) and chloroform was bought from Macron Fine Chemicals (U.S.). Moreover, Dulbecco's Phosphate Buffered Saline (DPBS) 0.0095M (PO4) without Ca and Mg and Trypsin-Versene (EDTA) of 170,000 U Trypsin/L were purchased by BioWhittaker® Lonza (Belgium). Glass Beads (acid-washed), Trypan Blue Solution (0.4%) and Thiazolyl Blue Tetrazolium Bromide were obtained from Sigma Aldrich.

Microcon® Centrifugal Filtrers from Merck Millipore (Darmstadt, Germany) were used for ultrafiltration of the digested rosemary extract. Filtropur S 0.2 syringe filters for sterile filtration without pre-filter (polyethersulfone-membrane, 0.2 μm pore size, 5.3 cm^2 filtration surface) were bought from Sarstedt (Nümbrecht, Germany). Moreover, the Pipet-Lite XLS+ Single Channel, Pipet-Lite XLS+ Multichannel and E4 XLS+ Single Channel were all purchased by Mettler Toledo (Switzerland). Finally, the Pipetus was obtained from Hirschmann (Germany), HSW 10 mL Soft-Ject™ Disposable Syringes were from Thermo Fisher Waltham (Massachusetts, USA) and the 15 mL Centrifuge Tubes were bought from VWR.

2.1.2. Rosemary extract and phenolic compound standards

The rosemary extract (RE) was obtained from dried rosemary leaves using supercritical CO_2 and 7% ethanol at 150 bar as reported by Herrero et al. [38]. Previous chemical characterization of the RE indicated that two main diterpenes, CA and CS, were found at high concentrations in the RE [38]. RE was dissolved at the indicated concentrations using ethanol prior to simulated digestion.

Phenolic compounds 12-O-Methylcarnosic acid (MCA) and rosmanol (RS) were bought from Phytolab (Germany), while carnosol (CS) and carnosic acid (CA) were from Sigma Aldrich.

2.1.3. Simulated gastrointestinal digestion

The digestion process in the gastrointestinal tract in humans was simulated in a simplified manner by applying physiologically based chemical composition of digestive fluids, pH and residence time periods typical for each compartment (stomach and gut). In this work, RE was subjected to a simulated digestion, which included the gastric and small intestinal phases, according to a standardized static *in vitro* digestion method suitable for food [21].

2.1.3.1. Gastric digestion

To imitate the gastric conditions, a simulated gastric fluid (SGF) was required. SGF (1.25× concentrated) was prepared by mixing the corresponding electrolyte stock solutions presented in **Table 2.1**.

Table 2.1. Preparation of 400 mL SGF (1.25x).

	SGF (1.25x)	
Electrolyte Stock solutions	**Volume (mL)**	**Final concentration (mM)**
KCl (0.5 M)	6.9	6.9
KH_2PO_4 (0.5 M)	0.9	0.9
$NaHCO_3$ (1 M)	12.5	25
NaCl (2 M)	11.8	47.2
$MgCl_2(H_2O)_6$ (0.15 M)	0.4	0.1
$(NH_4)_2CO_3$ (0.5 M)	0.5	0.5
HCl (1 M) for pH adjustment	1.3	15.6
Water	400 mL (final volume)	

The simulated gastric enzyme solution was prepared by dissolving porcine gastric mucosa pepsin in SGF (1.25x) at a concentration of 4 mg/mL. $CaCl_2$ was prepared in water at a concentration of 0.3 M. $CaCl_2$ is not initially added to the SGF (1.25x) solution as precipitation may occur. Before digestion, $CaCl_2$ was added to the gastric digestion solution to achieve a concentration of 0.075 mM. Prior to digestion, all solutions were filtered with 0.22 μm filter (Filtropur S 0.2 syringe filter) under sterile conditions. *In vitro* gastric digestion was carried out in 50 mL Falcon tubes by mixing the prepared simulated fluids and RE as indicated in **Table 2.2**.

Table 2.2. Preparation of 20 mL simulated gastric digestion solution.

Stock solutions	**Volume (mL)**
SGF (1.25x)	6.4
Water	10.695
$CaCl_2$ (0.3 M) in water	0.005
HCl (1 M) for pH adjustment	0.3
Pepsin (4 mg/mL) in SGF (1.25x)	1.6
RE (100 mg) in ethanol	1

The final gastric digestion solution was placed at 37 ºC, considered as the normal human body temperature, into a shaking incubator to provide the necessary mixing mimicking the peristaltic movements of stomach walls during digestion. The simulation of gastric digestion lasted two hours, a period representing the half emptying of stomach after

a moderately nutritious and semi-solid meal. The gastric digestion product of RE (GDP-RE) was then submitted to intestinal digestion. Additionally, an aliquot of the gastric digestion product was submitted to chemical characterization by UHPLC-TOF MS.

2.1.3.2. Intestinal digestion

Once the RE has been through the simulated gastric phase of digestion, it was transferred to a simulation of the digestion that occurs in the small intestine. A static steady value of pH 7 was selected through the neutralization of gastric chime in order to match the modifications of pH across the intestinal tract and the duration of two hours of the intestinal digestion simulation.

As we did for the gastric digestion, to mimic the small intestine conditions, a simulated gastric fluid (SIF) was used. SIF (1.25x concentrated) was prepared by mixing the corresponding electrolyte stock solutions presented in **Table 2.3.**

Table 2.3. Preparation of 400 mL SIF (1.25x).

	SIF (1.25x)	
Electrolyte Stock solutions	**Volume (mL)**	**Final concentration (mM)**
KCl (0.5 M)	6.8	6.8
KH_2PO_4 (0.5 M)	0.8	0.8
$NaHCO_3$ (1 M)	42.5	85
NaCl (2 M)	9.6	38.4
$MgCl_2(H_2O)_6$ (0.15 M)	1.1	0.33
HCl (1 M) for pH adjustment	0.7	8.4
Water	400 mL (final volume)	

$CaCl_2$ is not initially added to the SIF (1.25x) solution as precipitation may occur. $CaCl_2$ was added to the final small intestinal digestion solution to achieve a concentration of 0.3 mM. Bile salts (160 mM of fresh bile in water) were also added to obtain final concentration of 10 mM in agreement with the concentration found in the adult intestine in the fed state. Pancreatin from porcine pancreas, prepared at 800 U/mL) in SIF (1.25x) solution was added to reach final concentration of 100 U/mL in the intestinal digestion solution. Prior to digestion, all solutions were filtered with 0.22 μM filter under sterile conditions.

In vitro intestinal digestion was carried out in 50 mL Falcon tubes by mixing the prepared simulated intestinal fluids and the product from gastric digestion (**Table 2.4**).

Table 2.4. Preparation of 20 mL simulated intestinal digestion solution.

Stock solutions	**Volume (mL)**
Gastric product	10
SIF (1.25x)	5.5
Fresh bile (160 mM) in water	1.25
$CaCl_2$ (0.3M) in water	0.02
Pancreatin (800 U/mL) in SIF 1.25x	2.5
Water	0.73

The final intestinal digestion solution was incubated at 37 ºC for two hours. The gastrointestinal digestion product from RE (GI-RE) was submitted to sample preparation.

2.1.3.3. Sample preparation

GI-RE was submitted to different sample preparation procedures. First, digested solutions were centrifuged at 4,000 x g for 4 min. Obtained supernatant was submitted to filtration, ultrafiltration, and solid phase extraction (SPE). After sample preparation, aliquots from each sample treatment were stored at -80 ºC until cell culture assay and UHPLC-TOF MS analysis.

500 µL of the supernatant from GI-RE was filtrated using a 33 mm diameter sterile syringe filter with a 0.22 µm pore size PVDF membrane, and it was next stored at -80 ºC. 200 µL of the supernatant from GI-RE was ultrafiltrated by using 3 kDa Amicon Ultra 0.5 mL centrifugal devices from Merck Millipore (Darmstadt, Germany) at 14,000 × g for 30 min at 4 ºC. Fraction < 3 kDa from GI-RE was then stored at -80 ºC.

1 mL of the supernatant from GI-RE was submitted to SPE using 1 mL C18 cartridge (Supelco). Firstly, the SPE cartridge was conditioned with 3 mL of methanol (0.1% HCl), and then equilibrated with 5 mL of deionized water (0.1% HCl). Afterwards, the cartridge was loaded with 1 mL of the GI-RE and washed with 3 mL of deionized water (0.1% HCl). Phenolic compounds were eluted with 1 mL of ethanol (0.1% HCl) and stored at -80 ºC.

2.1.4. Total Phenols Content (Folin-Ciocalteu method)

The quantification of total phenols content (TPC) in the RE, GI-RE, SPE-treated (SPE/GI-RE), and ultrafiltrated GI-RE (U/GI-RE) was carried out using the Folin-Ciocalteu method with some modifications [39]. Briefly, 600 µL of water were mixed with 10 µL of each sample to which 50 µL of undiluted Folin-Ciocalteu reagent (2N) was subsequently added. After 1 min, 150 µL of 20% (w/v) Na_2CO_3 were added and the volume was made up to 1.0 mL with water. After 2 h of incubation at 25 ºC, 300 µL of the mixture was transferred into a well of a 96-well microplate. The absorbance was measured at 760 nm in a microplate spectrophotometer reader (Synergy HT, Bio Tek Instruments, Winooski, VT, USA). A gallic acid calibration curve (0.032-2.00 mg/mL) was elaborated in the same way and the TPC was expressed as mg of gallic acid (GAE) per g of extract. All analyses were done by triplicate.

2.1.5. Cell culture

Caco-2 cell lines were obtained from ATCC (American Type Culture Collection, LGC Promochem, UK). Caco-2 cells were grown in DMEM medium containing 10% (v/v) fetal bovine serum, 1% non-essential amino acid solution, 2 mM L-glutamine and 50 U/mL penicillin G and 50 U/mL streptomycin at 37 ^{o}C in humidified atmosphere and 5% CO2. Culture medium was replaced every 2 to 3 days.

2.1.6. Cytotoxicity assay on Caco-2 cells

MTT (3-(4,5-dimethyl-2-thiazolyl)-2,5-diphenyl-2H-tetrazolium bromide bromide) assay was performed on Caco-2 cells to determine the potential cytotoxic effects of RE, GI-RE, SPE/GI-RE, U/GI-RE samples, and the individual phenolic compounds, namely, CA, CS, RS and MCA, was tested by MTT assay. Briefly, cultured cells at ~50% confluence were trypsinized, neutralized with culture medium, seeded at 10,000 cells/cm^2, and allowed to adhere overnight at 37 °C. Thus, cells were treated with the vehicle (0.1% DMSO, v/v) regarded as untreated controls or with different concentrations of the samples under study, and incubated for 24 h. After treatments, cells were incubated with serum-free medium containing MTT (0.5 mg/mL) at 37 °C for 3 h. The medium was removed, and the purple formazan crystals were dissolved in DMSO. Then, the absorbance at 570 nm was

measured in a microplate reader (Synergy HT). The results are provided as the mean ± standard error of the mean (S.E.M.) of at least three replicates.

2.1.7. Transport experiment in Caco-2 monolayer

12-well plates with transwell membrane supports (Costar, USA) were used for the transport studies. Caco-2 cells were seeded on twelve-well transwells (1.12 cm^2 surface area) at a density of 1.5 x 10^5 cells/insert, and grown in Dulbecco's modified Eagle's medium (DMEM) with 10% fetal bovine serum, 1% non-essential amino acid solution, 50 U/mL penicillin G and 50 U/mL streptomycin, at 37°C with 5% CO_2. The medium was changed every 2/3 days. Cells were grown and differentiated to confluent monolayers for 21 days, as previously described [40]. All transport studies were conducted at 21st day post seeding.

2.1.7.1. Assessment of cell monolayer integrity

Each batch of monolayers was certified by measuring the transepithelial electrical resistance and the permeability of atenolol, propranolol and Lucifer yellow (LY).

During the period of growth and differentiation, the integrity of cell monolayers was examined every 2 to 3 days by measuring the transepithelial electrical resistance (TEER) with an EVOM^2 epithelial voltohmmeter from World Precision Instruments (FL, USA). The TEER-value was calculated as **Equation 2.1.:**

$$TEER\ [\Omega \times cm^2] = (R_{sample} - R_{blank}) \times A \qquad \textbf{(2.1.)}$$

Where R_{sample} [Ω] is the electrical resistance measured across the cell monolayer and R_{blank} [Ω] is the resistance of the insert without cells. A [cm^2] is the seeding area of the insert.

LY travel across cell monolayer only through paracellular diffusion and has low permeability. As a result it is not possible to cross cell monolayer when tight junctions are well maintained. The integrity of the monolayer was measured by monitoring LY, a paracellular marker across cell monolayer. 100 μM LY dissolved in HBSS was added to the apical chamber. After 1 h incubation, apical and basolateral solutions were collected. For LY quantification, the apical and basolateral solutions, together with LY at different concentrations to construct a calibration curve, were transferred to a 96 well black plate and read spectrophotometrically at 485/528 nm. %LY flux was determined, using the **Equation 2.2.**:

$$\%\text{LY Flux} = 100 \times \frac{[LY]_b/V_b}{[LY]_a/V_a} \qquad \textbf{(2.2.)}$$

Where $[LY]_b$ is the concentration of LY in the basolateral (receiver) chamber, V_b is the volume of the receiver chamber (1.5 mL), $[LY]_a$ is the concentration of LY in the apical (donor) chamber and V_a is the volume of the donor chamber (0.5 mL). % LY flux should be less or equal to 1%. Values lower than 1% indicated continuous good monolayer integrity in all passages.

The Caco-2 cell monolayer system was validated by examining the test compounds atenolol and propranolol at concentrations of 10 μM in HBSS at apical-to-basal compartments. After 2 h or 6 h incubation, apical and basolateral solutions were collected. For atenolol and propranolol determination, the apical and basolateral solutions were analyzed by UHPLC-TOF MS. Only the monolayers with integrity values comparable to published data were used.

2.1.7.2. Bi-directional transport study of phenolic compounds

Before and after each experiment, the physical integrity of the monolayer was certified by measuring the TEER. Only the monolayers with TEER > 300 Ω×cm^2 (subtracting the background value of a transwell) were considered for the transport assay.

All transport studies were conducted HBSS buffered (pH 7.0-7.4) at 37 °C. Cell monolayers were first washed three times with HBSS to remove any trace of culture medium. After washing, the plates were incubated with HBSS at 37 °C for 15 min and TEER was measured. In the study of transport, the RE and the GI-RE at non-cytotoxic concentrations were dissolved in HBSS to obtain the working solutions. Moreover, CA, CS, RS and MCA test solutions at non-cytotoxic concentrations, were also prepared in HBSS.

For the investigation of apical-basolateral transport (AP-BL), test compounds, RE and GI-RE were placed in the apical (0.5 mL) side and blank HBSS in the basolateral compartment (1.5 mL). Incubation was carried out for 6 h. Samples from the apical and basolateral compartments were collected at the beginning and at the end of each incubation period for UHPLC-TOF MS analyses.

For the investigation of basolateral-apical transport (BL-AP), test compounds, RE and GI-RE were placed in the basolateral (1.5 mL) side and blank HBSS in the apical compartment (0.5 mL). Incubation was carried out for 6 h. Samples from the apical and

basolateral compartments were collected at the beginning and at the end of each incubation period for UHPLC-TOF MS analyses.

2.1.7.3. Extraction of phenolic compounds from Caco-2 monolayer

The cells were detached from each well with a sterile rubber scraper. Transwell membrane supports were rinsed twice with 250 µL of HBSS. Cells were transferred to a vial and centrifuged for 5 minutes at 300 × g at 25 ^{o}C. After the centrifugation, the supernatant was discarded and the pellet was stored at -80 ^{o}C until metabolite extraction.

Metabolite extraction was carried out with 500 µL of precooled (-80 ºC) methanol containing 0.025 mM of *N*-Benzoyl-L-tyrosine ethyl ester as internal standard. Then, 0.3 g of glass beads were added to each vial and the cell extracts were homogenized with Mixer Mill at 30 Hz for 5 minutes. Cell extracts were centrifuged for 7 minutes at 6,000 × g at 4 ºC and 300 µL from the supernatant was evaporated to dryness using a nitrogen flow evaporator. Dried extracts were stored at -80 ^{o}C. Prior to UHPLC-TOF MS dried extracts were dissolved in 100 µL methanol-water (10:90 v/v).

2.1.7.4. Transport parameters calculation

The apparent permeability coefficient (P_{app}) was used as an expression of the absorption rate constant, and it was calculated using **Equation 2.3.**:

$$P_{app}=(dQ/dt)/(C_0A) \qquad \textbf{(2.3.)}$$

Where dQ/dt represents the rate of appearance of drug in the receiver chamber, A represents the membrane surface area of Caco-2 monolayer and C_0 is the initial drug concentration on the donor side.

The efflux ratio (EfR) for permeability was calculated as follows (**Equation 2.4.**):

$$EfR = P_{app\ BL\text{-}AP}/\ P_{app\ AP\text{-}BL} \qquad \textbf{(2.4.)}$$

Where with $P_{app\ BL\text{-}AP}$ and $P_{app\ AP\text{-}BL}$ are the mean permeability coefficients obtained for the basolateral-to-apical direction and apical-to-basolateral direction, respectively.

2.1.8. UHPLC-TOF MS conditions

All analyses were performed using an UHPLC Agilent 1290 Infinity LC system. Detection was performed with Agilent 6540 Ultra High Definition (UHD) Accurate-Mass Quadrupole Time-of-Flight (Q-TOF) LC/MS System equipped with Agilent Jet Stream (AJS) Electrospray Ionization (ESI) source. External calibration of the TOF MS was carried out using a commercial mixture from Agilent with next m/z values: 301.9981, 601.9790, 1,033.9881, 1,333.9689, 1,633.9498, 1,933.9306, 2,233.9115, 2,533.8923 and 2,833.8731. For data acquisition and analysis Agilent MassHunter Workstation software B.06.00 was used. The data were processed using Agilent Mass Hunter software version B.07.00. Extracted ion chromatograms of accurate masses for negative or positive ions were used for confirmation of the presence of phenolic compounds, as well as metabolites, within 10 ppm.

2.1.8.1. Phenolic profile determination

Separations were performed on a Hypersil gold C18 (50 x 2.1, 1.9 μm) column from Thermo Scientific, with a UHPLC Guard 3PK Zorbax SB-C8 (2.1 x 5.5 mm, 1.8 μm) precolumn from Agilent, to separate the compounds. The mobile phase consisted of (A) water with 0.1% formic acid, and (B) acetonitrile with 0.1% formic acid. Next gradient elution program was used: 0 min, 5% B; 0.35 min, 5% B; 3.5 min, 5% B; 6.2 min, 70% B; 9 min, 95% B. The column was equilibrated for 2 min prior to each analysis. The flow rate was set constant at 0.4 mL/min and injection volume was 2 μL. Each sample was analyzed in duplicate. MS parameters were the following: capillary voltage, 4,000 V; nebulizer pressure, 40 psi; drying gas flow rate, 10 L/min; gas temperature, 350 °C; skimmer voltage, 45 V; fragmentor voltage, 110 V. TOF MS accurate mass spectra were recorded across the range of 50-1,100 m/z at 1.5 spectra/s in negative ionization mode.

2.1.8.2. Atenolol and propranolol analysis

UHPLC-TOF MS was used for fast determination of atenolol and propranolol in the apical and basolateral chambers. Separations were performed on a Zorbax Eclipse Plus C18 Rapid Resolution HD (2.1x50 mm, 1.8 μm) column with a UHPLC Guard 3PK Zorbax SB-C8 (2.1x5.5 mm, 1.8 μm) precolumn, both from Agilent. The mobile phase consisted of (A) water with 0.1% formic acid, and (B) acetonitrile with 0.1% formic acid.

Next gradient elution program was used: 0 min, 10% B; 1.5 min, 95% B; 2 min, 95% B. The column was equilibrated for 2 min prior to each analysis. The flow rate was set constant at 0.6 mL/min and injection volume was 2 μL. Each sample was analyzed in duplicate. MS parameters were the following: capillary voltage, 4000 V; nebulizer pressure, 40 psi; drying gas flow rate, 10 L/min; gas temperature, 350 °C; skimmer voltage, 45 V; fragmentor voltage, 110 V. TOF MS accurate mass spectra were recorded across the range of 50-1,100 m/z at 1.5 spectra/s in positive ionization mode.

2.1.8.3. Analysis of phenolic compounds

Analysis of phenolic compounds at the apical and basolateral compartments was performed on a Zorbax Eclipse Plus C18 Rapid Resolution HD (2.1x50 mm, 1.8 μm) column with a UHPLC Guard 3PK Zorbax SB-C8 (2.1x5.5 mm, 1.8 μm) precolumn, both from Agilent. The mobile phase consisted of (A) water with 0.1% formic acid, and (B) acetonitrile with 0.1% formic acid. Next gradient elution program was used: 0 min, 5% B; 1 min, 60% B; 2.3 min, 60% B; 3 min, 95% B; 5 min, 95% B. The column was equilibrated for 2 min prior to each analysis. The flow rate was set constant at 0.6 mL/min and injection volume was 2 μL. Each sample was analyzed in duplicate. MS parameters were the following: capillary voltage, 4000 V; nebulizer pressure, 40 psi; drying gas flow rate, 10 L/min; gas temperature, 350 °C; skimmer voltage, 45 V; fragmentor voltage, 110 V. TOF MS accurate mass spectra were recorded across the range of 50-1,100 m/z at 1.5 spectra/s in negative ionization mode.

The gradient elution program for the analysis of phenolic compounds at the intracellular Caco-2 fraction was slightly modified to avoid carryover between samples. Thus, gradient elution program used was next: 0 min, 5% B; 1 min, 60% B; 2.3 min, 60% B; 3 min, 100% B; 6 min, 100% B. Other UHPLC-TOF MS conditions were the same.

2.2. RESULTS AND DISCUSSION

2.2.1. Chemical characterization of gastrointestinal digestion of RE

In order to evaluate the stability of phenolic compounds during their passage through the gastro-intestinal (GI) digestion, an *in vitro* method was used that simulates GI conditions that food components undergo during digestion. After this simulation, gastro-intestinal digestion product from RE (GI-RE) was centrifuged to remove debris and directly analyzed by UHPLC-TOF MS for its chemical characterization.

In **Figure 2.1.** the total ion chromatogram (TIC) and the extracted ion chromatograms (EICs) of the main phenolic compounds observed in the RE (black line) and GI-RE (pink line), are showed.

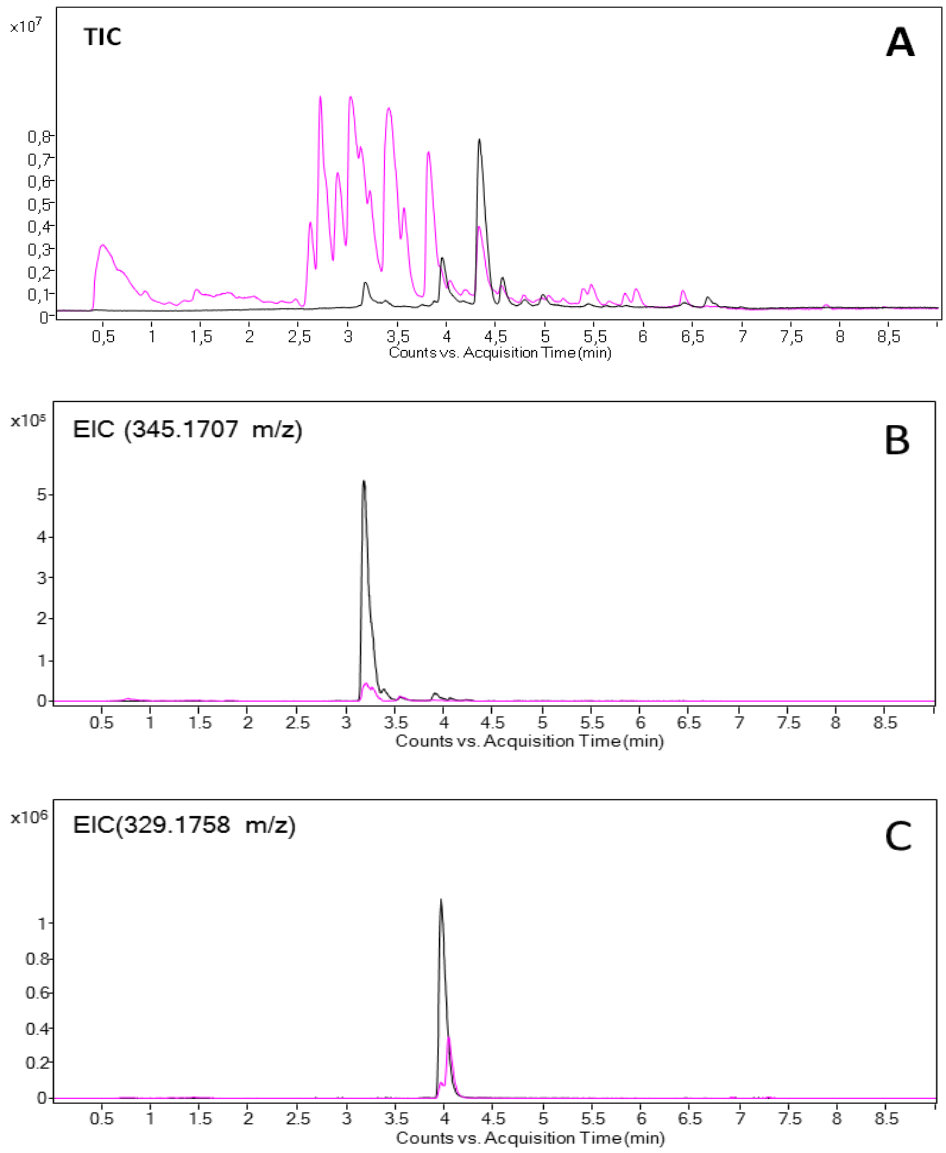

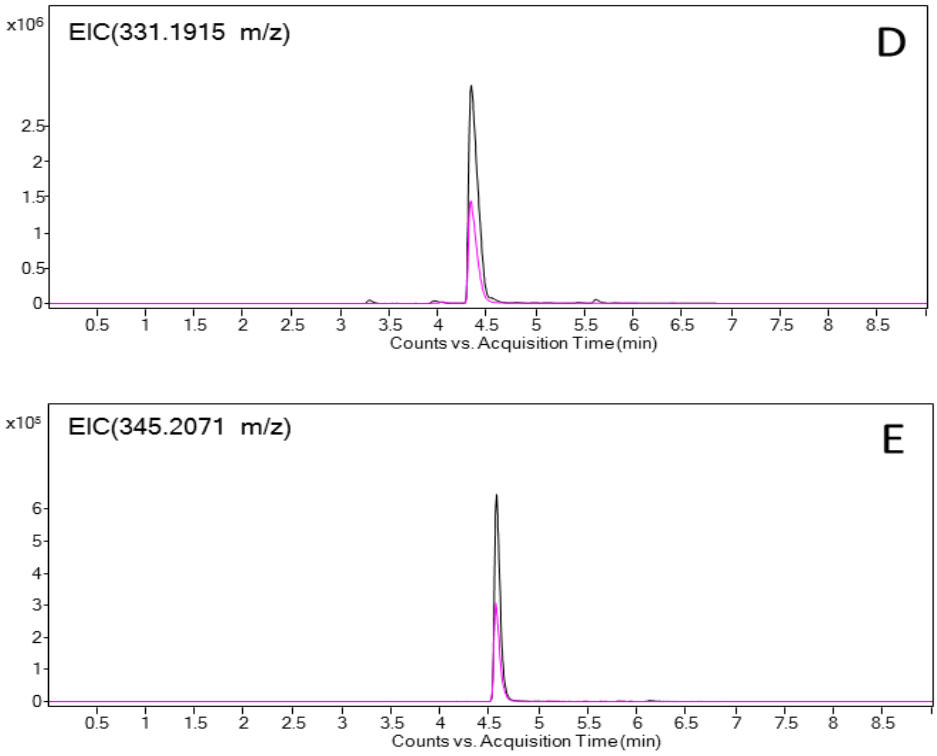

Figure 2.1. *Analysis of RE (black chromatograms) and GI-RE (pink chromatograms).* ***A****: Total ion chromatogram;* ***B****: EICs of RS (345.1707 m/z);* ***C****: EICs of CS (329.1758 m/z);* ***D****: EICs of CA (331.1915 m/z);* ***E:*** *EICs of MCA 345.2071 m/z).*

As can be seen in **Figure 2.1.** the main phenolic compounds in RE are RS, CS, CA and MCA. After GI digestion, peaks corresponding to these diterpenes were observed to be decreased. The percentage of remaining RS, CS, CA and MCA were 11.9±0.1%, 5.8±0.1%, 44.3±0.6% and 49.50±0.03%, respectively. A new peak corresponding to carnosic acid quinone (CA-Q) appeared after GI digestion (**Figure 2.1.C**). CA-Q is known to be the intermediate in the degradation pathway of CA [41]. These results indicate an important loss of phenolic compounds during gastrointestinal digestion, most probably due to degradation processes and protein-phenolic compounds that may induce formation of precipitates [42].

At **Table 2.5.** the chromatographic and mass characteristics of the main phenolic compounds in RE are presented.

Table 2.5. Chromatographic and mass characteristics of the main phenolic compounds in RE.

Peak name	Compound	RT (min)	Molecular formula	$[M-H]^-$
RS	Rosmanol	3.20	$C_{20}H_{26}O_5$	345.1707
CS	Carnosol	3.96	$C_{20}H_{26}O_4$	329.1758
CA-Q	Carnosic acid quinone	4.04	$C_{20}H_{26}O_4$	329.1758
CA	Carnosic acid	4.34	$C_{20}H_{28}O_4$	331.1915
MCA	12-O-Methylcarnosic acid	4.57	$C_{21}H_{30}O_4$	345.2071

2.2.2. Cytotoxicity of RE and digestion products

As it has been discussed above, we observed a general loss of soluble phenolic compounds during the simulated GI of RE. Such dilution effect of the phenolic compounds in the gastrointestinal fluid limited its subsequent cytotoxicity testing on Caco-2 cells. This situation was aggravated by the observed cytotoxic effect of gastrointestinal fluids (GI-control) in Caco-2 cells (**Figure 2.2.**). As it is shown in the figure, the three tested dilutions of gastrointestinal fluid were highly toxic to Caco-2 cells, and a concentration-dependent reduction of Caco-2 cell viability with the GI-control sample can be observed. This effect may be likely due to the presence of high concentrations of biliary salts and digestive enzymes in the digestion fluid that may exert *in vitro* toxic effects.

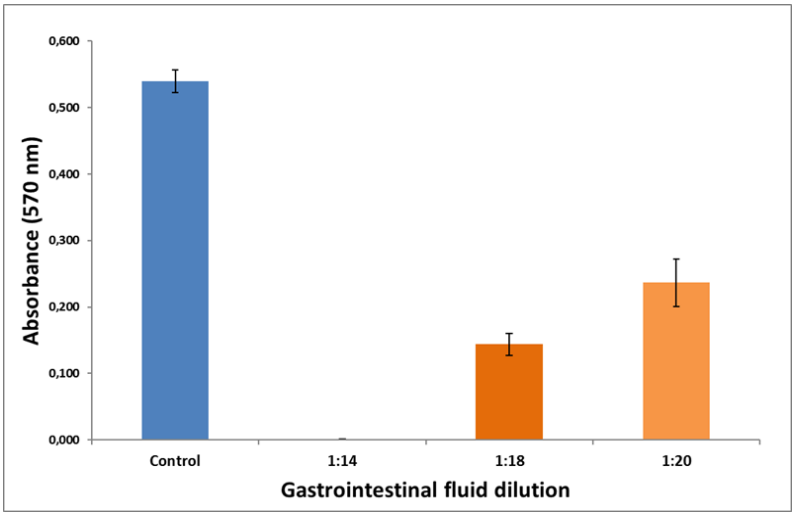

Figure 2.2. *Cytotoxic effect of gastrointestinal fluid for 24 h. Three different dilutions (1:14, 1:18, and 1:20; v/v) of filtered (0.22 µm) GI-control samples were prepared in culture medium and tested on Caco-2 cells using MTT assay. Error bars are given as the standard error of the mean (S.E.M.) of three replicates.*

In order to eliminate those cytotoxic interfering compounds that could potentially obscure the cytotoxic effect of rosemary compounds in GI-RE samples in the MTT assay, the purification of GI-RE samples was approached following two different sample preparation strategies, based on SPE and ultrafiltration, respectively (see **Section 2.1.3.3** for details).

Total phenols content was then quantified in RE, filtered (0.22 μm) GI-RE and GI-control samples, and purified fractions (SPE/GI-RE and U/GI-RE) using Folin-Ciocalteu method as described in experimental section (see **Section 2.1.4** for details). As can be observed in **Table 2.6**, the total phenol value for RE was 144.17 mg GAE/g extract.

Table 2.6. Total phenol content of RE and SPE/GI-, Filtered GI-, U/GI-samples and controls.

	Total phenol (mg of GAE/g extract)		
Sample	**Control**	**RE**	**Difference**
RE		144.17	
SPE/GI-	0.159 ± 0.003	0.416 ± 0.033	0.257
Filtered GI-	0.407 ± 0.003	0.605 ± 0.012	0.198
U/GI-	0.343 ± 0.013	0.414 ± 0.014	0.071

The analysis of the GI-control samples revealed that some compounds in digestion fluids interfered with Folin-Ciocalteu reaction.

SPE seemed to be the most effective procedure for interfering compounds removal as deduced by the low values observed in SPE/GI-control sample (0.159 mg GAE/mL). After subtracting the signal obtained for SPE/GI-control, among the all GI-RE samples tested, SPE/GI-RE sample exhibited the highest total phenol value (0.257 mg GAE/mL).

The analysis of filtered (0.22 μm) GI-RE sample showed lower total phenol content (0.198 mg GAE/mL) than in SPE/GI-RE sample. It can be seen that filtered GI-control sample gave the higher value (0.407 mg GAE/mL), what indicates that after filtration with 0.22 μm membrane still important fraction of compounds from GI digestion fluids interfered with Folin-Ciocalteu reaction.

Ultrafiltration procedure was not as effective as SPE for the interfering compounds removal, and the amount of remaining phenolic compounds in digested RE samples after ultrafiltration was lower (0.071 mg GAE/mL) compared with the other procedures.

Altogether, these results indicate that SPE procedure provided best results in terms of purification of phenolic compounds from digested RE samples.

Next, the effects of purified samples were tested on cell viability using MTT assay. To achieve this three dilutions (1:100, 1:125, and 1:250, v/v) of SPE/GI-RE and control samples were prepared in culture medium and tested on Caco-2 cells. As it is shown in **Figure 2.3.**, none of the assayed SPE/GI-control dilutions affected significantly cell viability, whereas SPE/GI-RE dilutions 1:100 and 1:125, corresponding to 2.6 µg and 2.1 µg GAE/mL showed only a mild effect on cell viability.

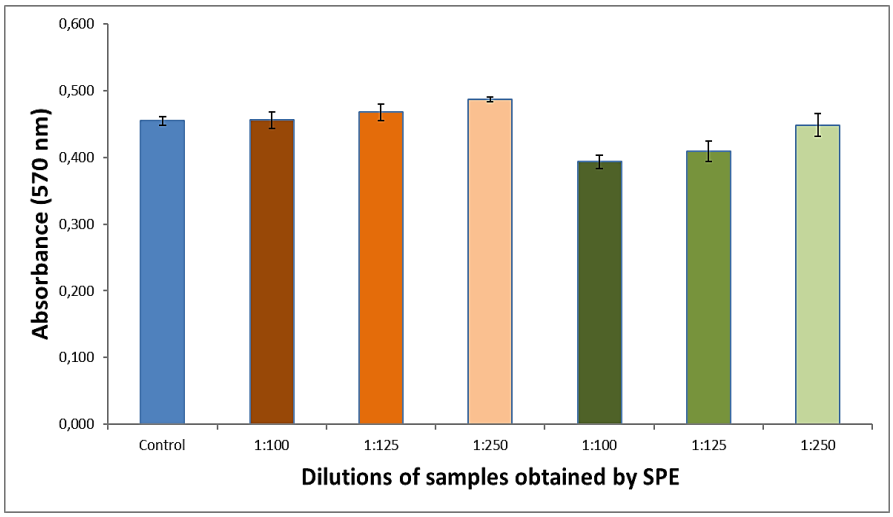

Figure 2.3. *MTT values obtained from the 24 h-exposure of Caco-2 cells to different dilutions of SPE samples: SPE/GI-control (orange bars); and SPE/GI-RE (green bars). Error bars are given as the standard error of the mean (S.E.M.) of three replicates.*

On the other hand, to test the toxic potential of purified control samples obtained by ultrafiltration procedure, three different dilutions (1:20, 1:40 and 1:80, v/v) of U/GI-control samples were prepared in culture medium and subsequently tested on Caco-2 cells by MTT assay. As can be observed in **Figure 2.4.A**, U/GI-control did not exert cytotoxic effects at any of the dilutions tested. Next, we tested same dilutions of U/GI-RE samples. Similarly to the results obtained with SPE samples, the three dilutions of U/GI-RE samples, 1:20, 1:40, and 1:80 (equivalent to 3.5, 1.8 and 0.9 µg GAE/mL, respectively) did not reduced Caco-2 cell viability (**Figure 2.4.B)**.

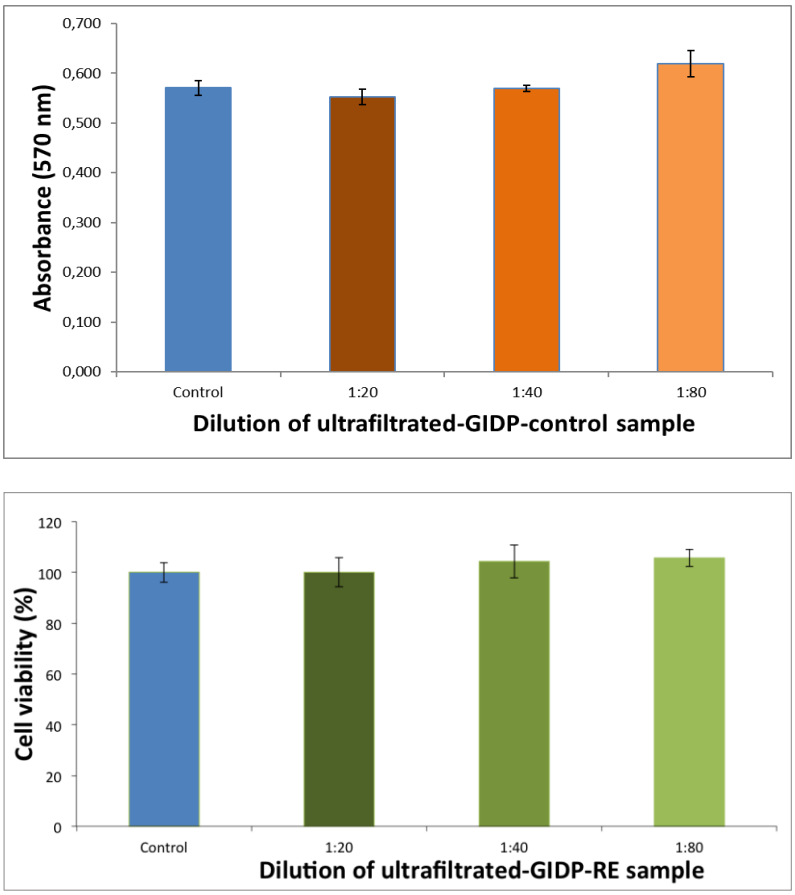

Figure 2.4. *MTT values obtained from the 24 h-exposure of Caco-2 cells to different dilutions of (A) U/GI-control (orange bars) and (B) U/GI-RE (green bars). Error bars are given as the standard error of the mean (S.E.M.) of three replicates. Error bars are given as the standard error of the mean (S.E.M.) of three replicates.*

In order to compare the cytotoxicity of purified digested RE samples with that exerted by RE on Caco-2 cell line, cells were incubated with increasing concentrations of the RE (3.8-60.0 µg/mL) for 24 h, and cell viability was analyzed by the MTT assay. As it is shown in **Figure 2.5.**, a concentration-dependent reduction of cell viability was observed starting from 30 µg/mL RE after 24 h of incubation. These results are similar to previous results obtained in our laboratory for the same extract on other colon cancer cell lines [43].

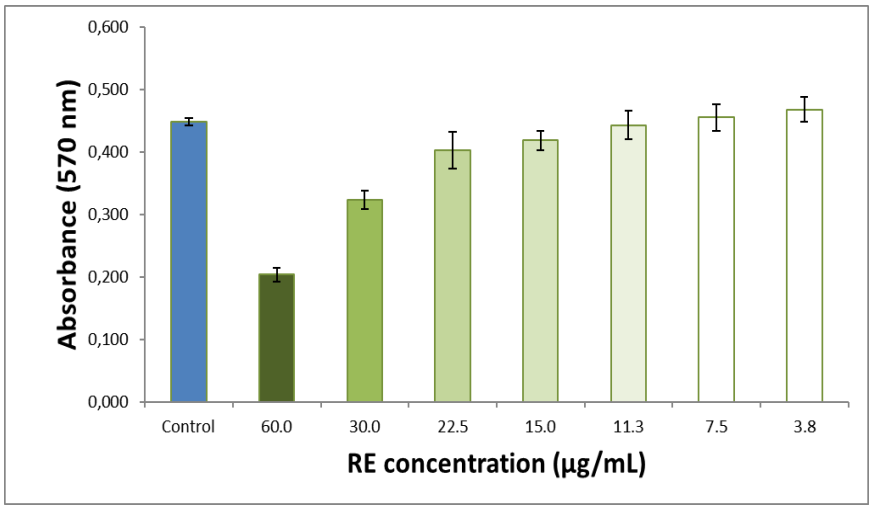

Figure 2.5. *Caco-2 viability upon treatment after 24 h with different concentrations of RE. Error bars are given as the standard error of the mean (S.E.M.) of three replicates.*

Interestingly, the concentration of 30 µg/mL RE, that exerts approximately a 30% cell viability reduction, was calculated to contain 4.3 µg GAE/mL, which is slightly lower than 3.5 µg GAE/mL calculated for the lowest dilution of U/GI-RE, suggesting that phenolic composition in RE is more bioactive in terms of cytotoxicity than in the ultrafiltrated sample. By contrast, total phenolic content is higher in 30 µg/mL RE than in the lowest SPE/GI-RE dilution assayed (2.5 µg GAE/mL). Such dilution has shown to exert approximately a 10% cell viability reduction, suggesting that the phenolic composition in RE is less bioactive in terms of cytotoxicity than in the SPE/GI-RE sample. These contrasting results indicate that composition among both, SPE/GI-RE and U/GI-RE samples might be different, not only in total phenolic content, but also in terms of individual phenolic compounds. Thus, SPE/GI-RE and U/GI-RE were analyzed by UHPLC-TOF to analyze the changes in the phenolic profile.

After UHPLC-TOF MS analysis, differences in phenolic profiles could be observed (**Figure 2.6.**) between SPE/GI-RE (dark blue line) and U/GI-RE (light blue line).

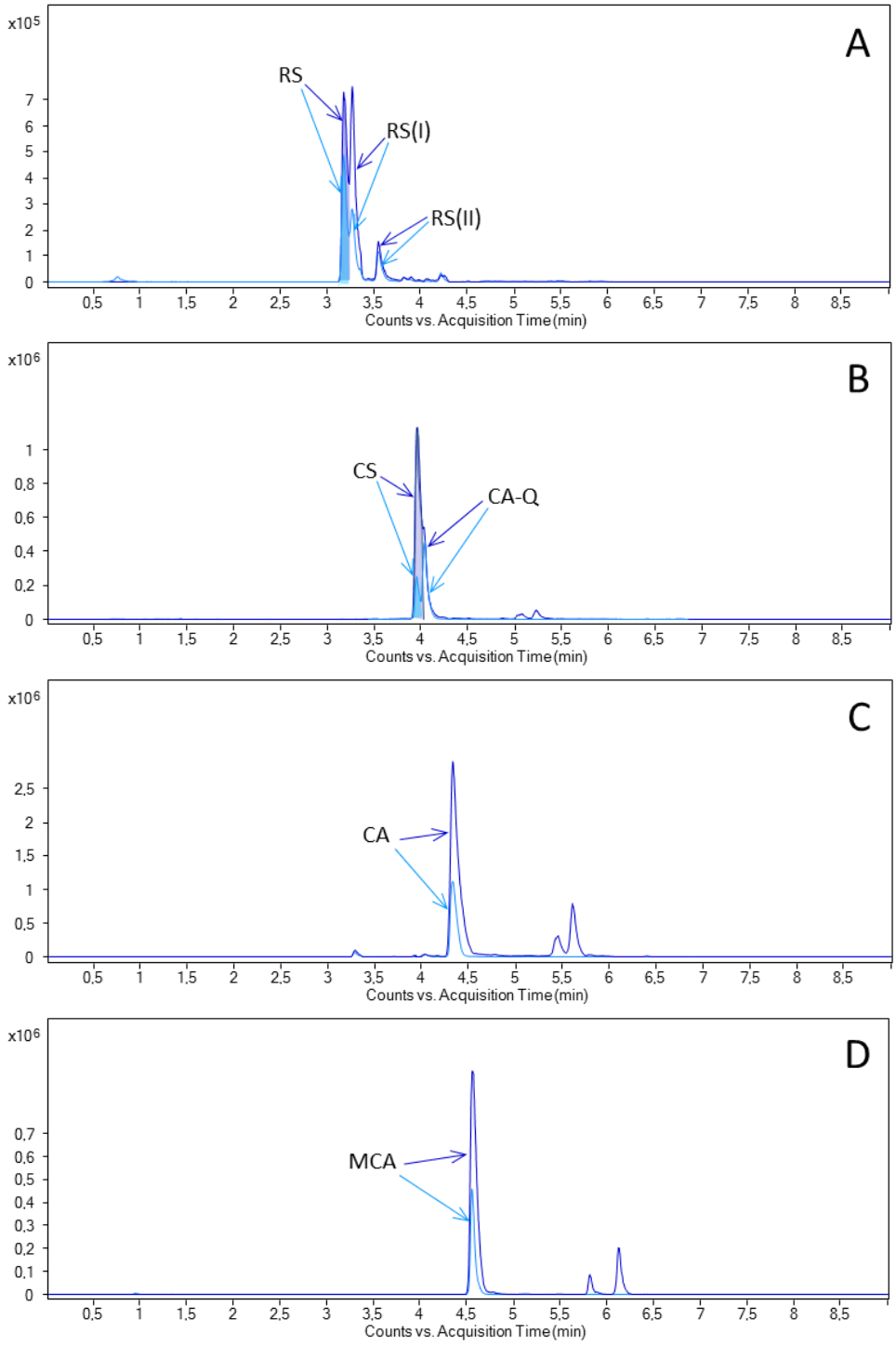

Figure 2.6. *Extracted ion chromatograms of RS (345.1707 m/z), CS (329.1758 m/z), CA (331.1915 m/z) and MCA (345.2071 m/z), in SPE/GI-RE (dark blue line) and U/GI-RE (light blue line).*

As it can be seen, differences in the main phenolic compounds were observed. In general, lower content of phenolic diterpenes RS, CS, CA and MCA were detected in U/GI-RE. After ultrafiltration, the % remained RS, CS, CA and MCA were 65.9±0.8%,

16.2±1.2%, 29.3±0.8% and 32.79±0.05%, respectively. Moreover, in **Figure 2.6.A**, three different peaks with same m/z (345.1707 m/z) were detected. In addition to RS, epirosmanol (RS I) and epiisorosmanol (RS II) could be detected. Identification was achieved by comparison of experimental and theoretical exact mass and retention time obtained in previous work [44]. CA-Q was also detected in both U/GI-RE and SPE/GI-RE samples (**Figure 2.6.B**).

2.2.3. Cytotoxicity of phenolic compound standards

As a previous step before permeability assay of the rosemary diterpenes CA, CS, RS and MCA, it was established to use a subtoxic concentration of each compound. To derive these values for Caco-2 cell line, cytotoxicity tests were performed. MTT assays were conducted to determine the cytotoxic effect of the rosemary diterpenes (CA, CS, RS and MCA) on Caco-2 cells. Cells were treated with different concentrations (10-100 μM) of the diterpenes and incubated for 24 h at 37 °C and 5% CO_2. As can be observed, all the diterpenes exhibited a concentration-dependent cytotoxic effect after 24 h (**Figure 2.7.**). Results indicated that CA (**Figure 2.7.A**) and CS (**Figure 2.7.B**) showed a similar cytotoxic activity on Caco-2 cells. Among the four assayed diterpenes, RS (**Figure 2.7.C**) was the most potent reducing cell viability whereas MCA acid showed the lowest cytotoxic activity (**Figure 2.7.D**). In general, concentrations below 25 μM do not appear to have significant effects; therefore, 20 μM diterpene was selected as subtoxic concentration for further transport experiments using Caco-2 cell monolayers.

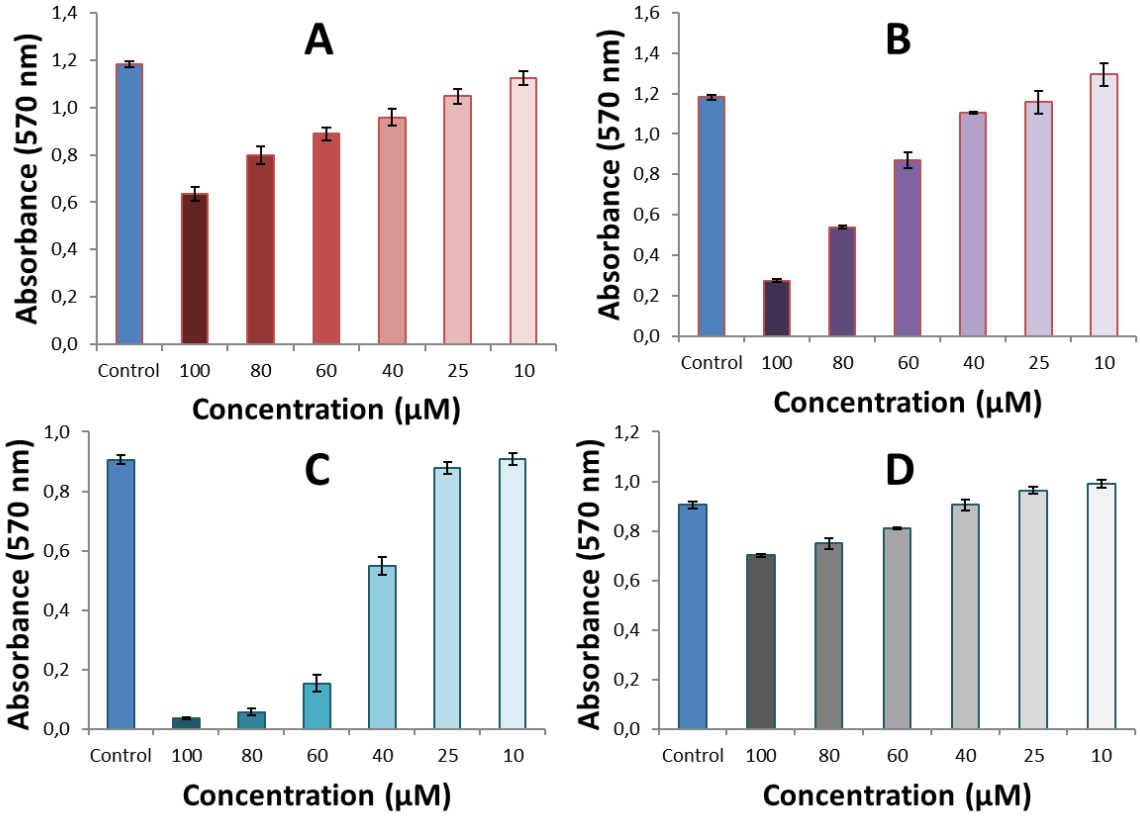

Figure 2.7. *Caco-2 viability upon treatment for 24 h with different concentrations of (A) CA, (B) CS, (C) RS, and (D) MCA. Error bars are given as the standard error of the mean (S.E.M.) of three replicates.*

2.2.4. Transport assay

The Caco-2 cell line has been widely used as a model of intestinal absorption and estimate of oral bioavailability. This cell line thus represents an appropriate model for the study of transport mechanisms related to the intestinal barrier. Bi-directional apical-to-basolateral (AP-BL) and basolateral-to-apical (BL-AP) direction transport of four diterpenes (CA, CS, RS and MCA) across Caco-2 cell monolayers was examined as pure compound and from RE and GI-RE.

2.2.4.1. Validation of the Caco-2 monolayers

To validate the Caco-2 cell monolayer system, the P_{app} values of atenolol and propranolol from the AP to the BL across the Caco-2 monolayers were determined (**Table 2.7.**).

Table 2.7. Caco-2 cell permeability of model drugs for Caco-2 monolayer system suitability.

Compound	Class[a]	Human intestinal absorption[b]	P_{app} ($x10^{-6}$ cms^{-1})	
			t=2h	t=6h
Atenolol	Class III (high solubility, low permeability)	50%	0.18±0.017	0.56±0.033
Propranolol	Class I (high solubility, high permeability)	90-95%	7.6±1.6	14.3±0.26

[a] Biopharmaceutics classification system [45].

[b] Human intestinal absorption values were obtained from the literature [25, 46].

These values were in good agreement with those published in previous reports [26, 47, 48] and thus, Caco-2 monolayer system was considered suitable for permeability study.

2.2.4.2. Bi-directional transport of test compounds in Caco-2 monolayer

2.2.4.2.1. Stability of phenolic compounds

Bi-directional AP-BL and BL-AP transport experiments of individual test compounds CS, CA, RS and MCA across Caco-2 cell monolayers were carried out.

First, stability of CS, CA, RS and MCA at the donor compartment was addressed. For this experiment, CS, CA, RS and MCA were placed in the apical compartment and blank HBSS in the basolateral compartment, and incubated in presence and absence of Caco-2 monolayer. Samples from the apical compartment were collected at the beginning and at the end of incubation (6 h) and UHPLC-TOF MS was employed to detect RS, CS, CA, and MCA and their degradation products in the apical chamber.

Figure 2.8. shows the results % of diterpenes remaining in apical chamber in absence of Caco-2 cells (dark green bar) and in presence of Caco-2 cells (light green bar) after 6 h incubation.

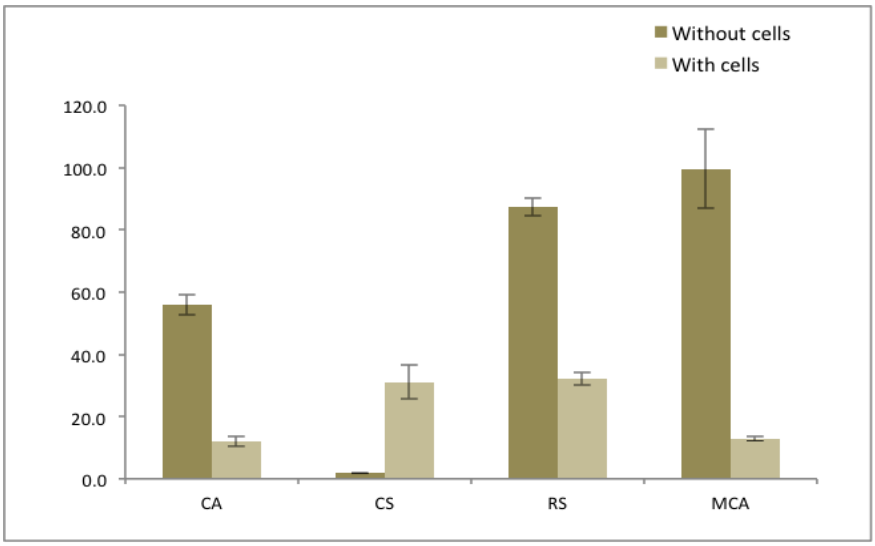

Figure 2.8. *% of CA, CS, RS and MCA incubated in HBSS for 6 h in absence of Caco-2 cells (dark green bar) and in presence of Caco-2 cells (light green bar).*

In absence of Caco-2 cells, the percentage of remaining CA, CS, RS and MCA were 56.0±3.3%, 1.8±0.1%, and 87.4±2.8%, 99.7±12.8, respectively.

CS exhibited a remarkable behavior: after 6 h of incubation only 1.8% CS remained in the HBSS medium. However, in presence of the Caco-2 monolayer, 31.1% CS remained in the HBSS medium after 6 h incubation. It is hypothesized that CS loss may arise from degradation (see below) and from interactions with plastic surface of wells; however, further experiments are required to confirm this point. On the contrary, MCA was totally stable after 6 h incubation in HBSS. The analysis of extracellular media (in presence of Caco-2 monolayer) revealed the Caco-2 uptake of CA, RS and MCA, with 12.0±1.5%, 32.0±2.0% and 12.9±0.7% remaining in extracellular medium.

After the analysis of the incubated diterpenes solutions in absence of cells, different degradation products were observed. **Figure 2.9.** shows the UHPLC-TOF MS analysis before and after incubation of CA.

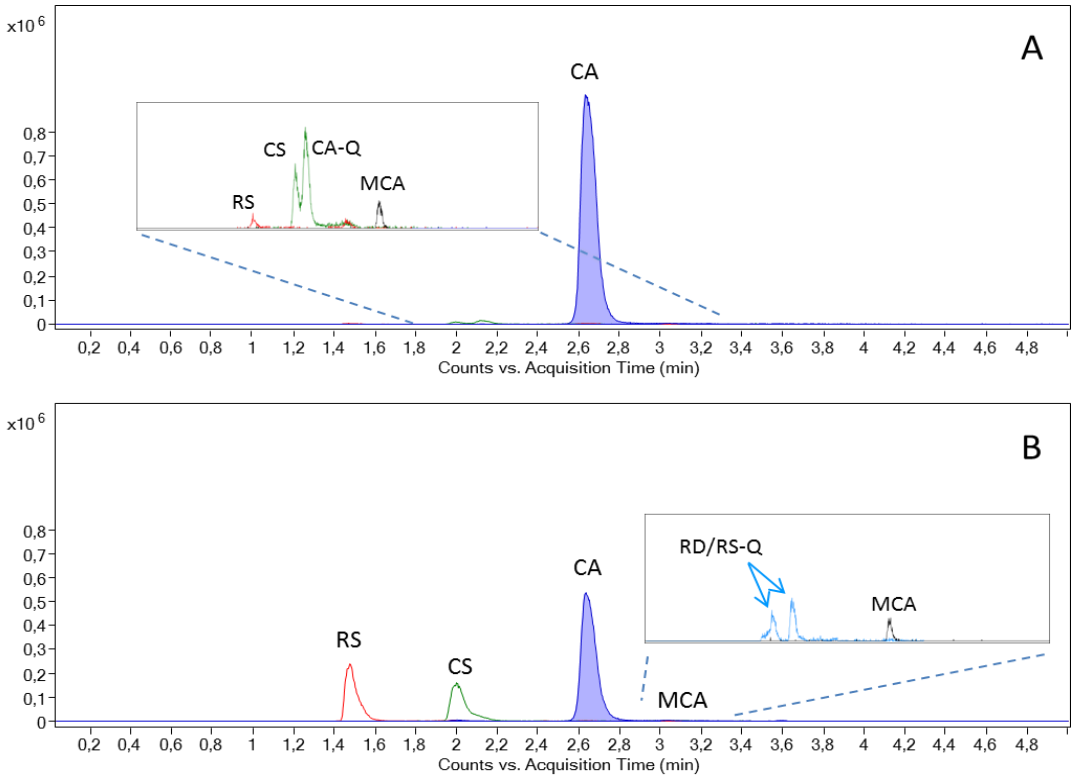

Figure 2.9. *Extracted ion chromatograms of RS (345.1707 m/z, red line), CS (329.1758 m/z, green line), CA (331.1915 m/z, blue line), MCA (345.2071 m/z, black line), rosmadial (RD) (345.1707 m/z, light blue) and rosmanol quinone (RS-Q) (345.1707 m/z, light blue), before (A) and after (B) incubation in absence of cells.*

As can be seen, in the incubations performed with CA, main degradation products were CS and RS. Rosmadial (RD) and rosmanol quinone (RS-Q) were also found. MCA was detected before and after incubation of CA. This is most probably due to impurities in the CA commercial standard. Traces of CA-Q were also detected. CA-Q was very likely to be the intermediate in the degradation pathway of CA. **Figure 2.10.** shows the UHPLC-TOF MS analysis before and after incubation of CS.

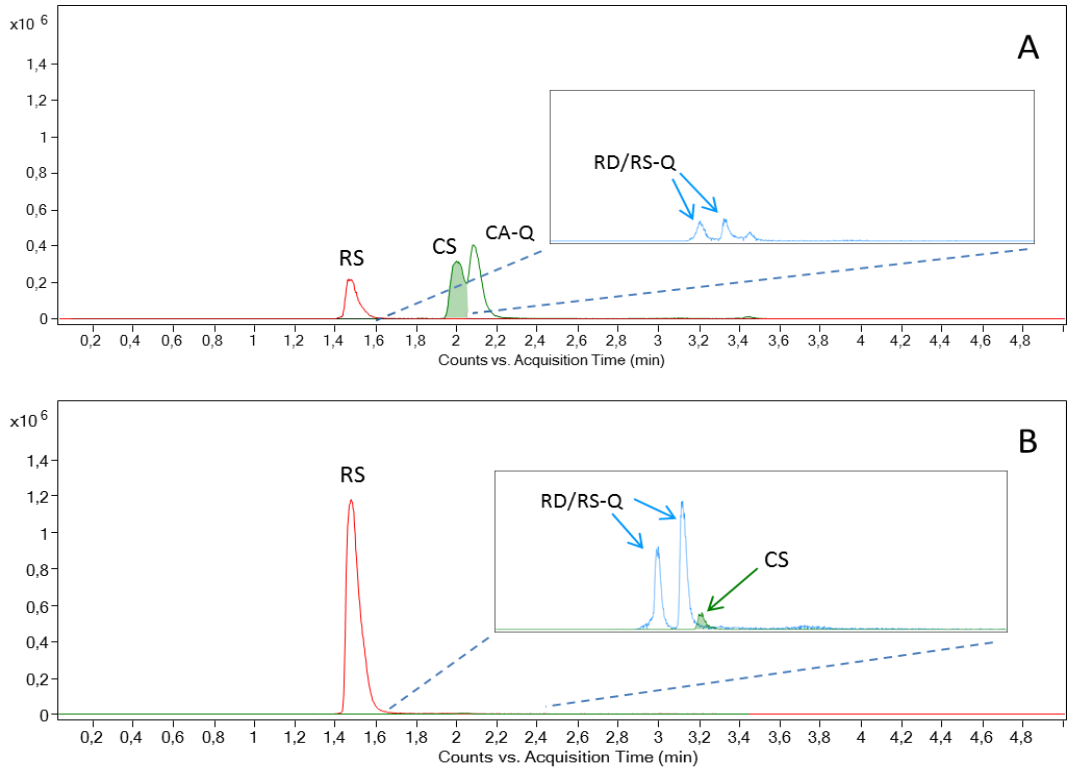

Figure 2.10. *Extracted ion chromatograms of RS (345.1707 m/z, red line), CS (329.1758 m/z, green line), rosmadial (RD) (345.1707 m/z, light blue) and rosmanol quinone (RS-Q) (345.1707 m/z, light blue), before (A) and after (B) incubation in absence of cells. CA and MCA were not observed.*

It can be observed that before incubation, an unexpected peak corresponding to CA-Q was observed. This may be due to CA-Q impurity in CS commercial standard. CA-Q by-product formation during the manufacture of CS standard from raw material containing CA was hypothesized to explain the presence of CA-Q in commercial preparations. Further investigation is required to confirm this point. It can also be observed that main degradation product of CS was RS. Rosmadial (RD) and rosmanol quinone (RS-Q) were also found to be increased after 6 h of incubation, but compared with RS, peak area of RD and RS-Q were very low. **Figure 2.11.** shows the UHPLC-TOF MS analysis before and after incubation of RS.

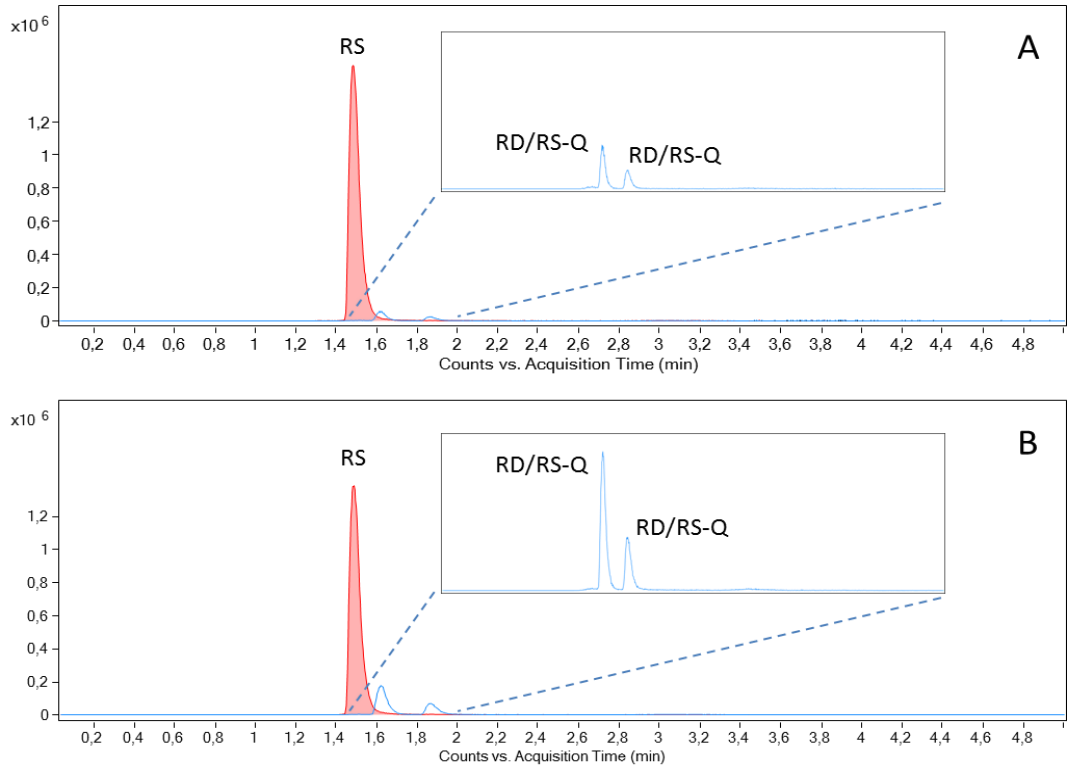

Figure 2.11. *Extracted ion chromatograms of RS (345.1707 m/z, red line), rosmadial (RD) (345.1707 m/z, light blue) and rosmanol quinone (RS-Q) (345.1707 m/z, light blue), before (A) and after (B) incubation in absence of cells. CA, CA and MCA were not observed.*

After 6 h incubation in HBSS, the percentage of remaining RS was 87.4%, and main degradation products were RD and RS-Q. **Figure 2.12.** shows the UHPLC-TOF MS analysis before and after incubation of CS.

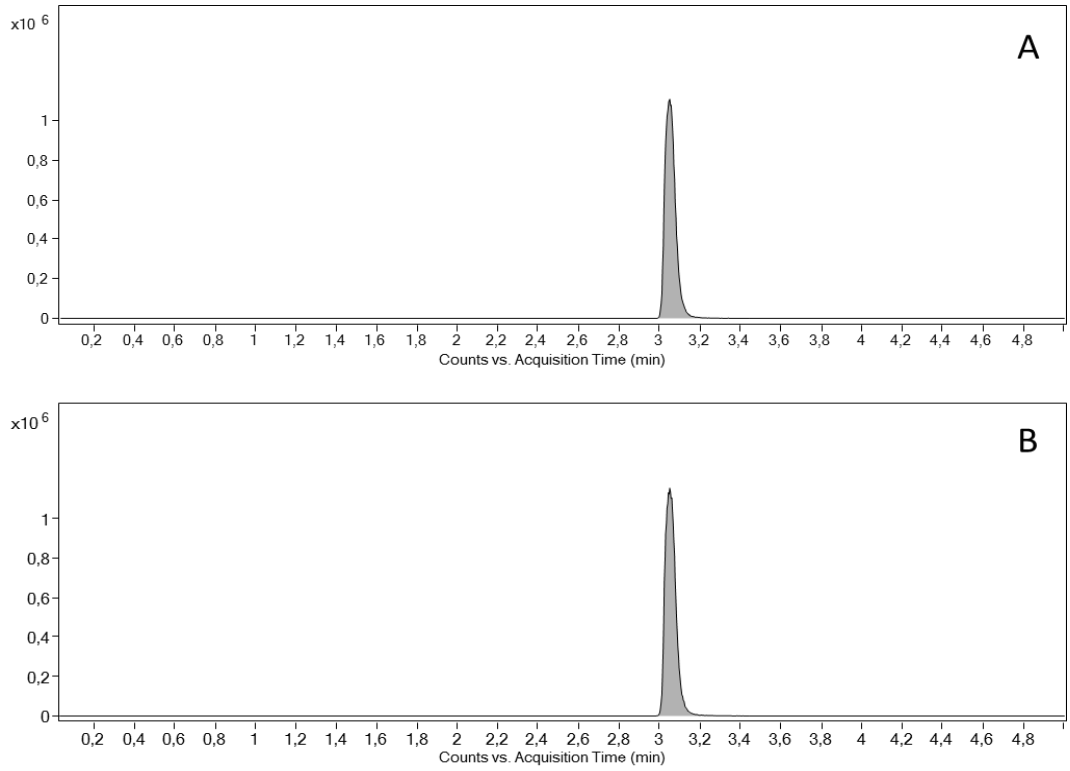

Figure 2.12. *Extracted ion chromatograms of MCA (345.2071 m/z, black line), before (A) and after (B) incubation in absence of cells. Other compounds were not observed.*

No degradation products were observed after the incubation of MCA during 6 h in absence of Caco-2 cells, in good agreement with the 99.7% of remaining MCA after incubation.

Several works have been previously published regarding the degradation of phenolic diterpenes from rosemary under different conditions [41, 49].

At **Table 2.8.** the chromatographic and mass characteristics of rosemary phenolic compounds and their degradation products are shown.

Table 2.8. Chromatographic and mass characteristics of phenolic diterpenes from rosemary and their degradation products.

Peak name	Compound	RT (min)	Molecular formula	$[M-H]^-$
RS	Rosmanol	1.44	$C_{20}H_{26}O_5$	345.1707
RD/RS-Q	Rosmadial/ Rosmanol quinone	1.61	$C_{20}H_{24}O_5$	343.1551
RD/RS-Q	Rosmadial/Rosmanol quinone	1.85	$C_{20}H_{24}O_5$	343.1551
CS	Carnosol	2.04	$C_{20}H_{26}O_4$	329.1758
CA-Q	Carnosic acid quinone	2.18	$C_{20}H_{26}O_4$	329.1758
CA	Carnosic acid	2.76	$C_{20}H_{28}O_4$	331.1915
MCA	12-O-Methylcarnosic acid	3.09	$C_{21}H_{30}O_4$	345.2071

Figure 2.13. shows the oxidation cascade of CA, a series of chemical reactions by which CA is converted to CS and CS is subsequently converted to RS. Being the predominant phenolic antioxidant in rosemary, CA is the starting element in this unique cascade mechanism. CA molecule extracts a free radical and it is converted to CS, which molecule also extracts a free radical and it is converted to RS. More specifically, CA is oxidized to CA-quinone. The intermediate CA-quinone undergoes rearrangement to CS. Dehydrocarnosic acid can also be produced from CS and it is further oxidized through quinone-semiquinone intermediates to RS.

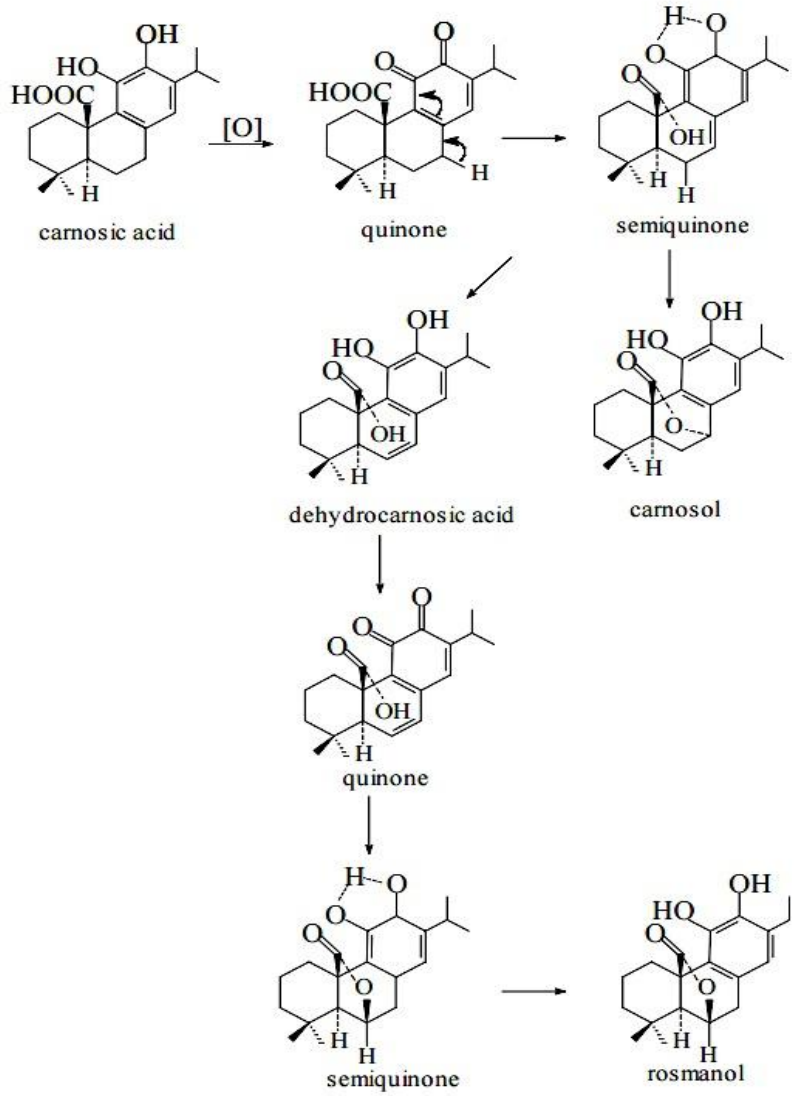

Figure 2.13. *Cascade mechanism in the oxidation reactions of CA [49].*

2.2.4.2.2. Bi-directional permeability of phenolic compounds from rosemary in Caco-2 monolayer

Next, transport of individual compounds (RS, CS, CA, and MCA) was evaluated, and P_{app} values were determined for each standard compound across Caco-2 cell monolayers. For the permeability experiment, test compounds, RE and GI-RE were placed in the donor chamber (apical or basolateral) and blank HBSS in the receiver compartment and incubated in presence and absence of Caco-2 monolayer. Samples from the apical and basolateral compartments were collected at the beginning and at the end of incubation period and analyzed UHPLC-TOF MS to detect RS, CS, CA, and MCA. The following **Figure 2.14.** shows typical extracted ion chromatograms (EICs) from standard compounds RS, CS, CA, and MCA in the AP-BL direction experiment across the Caco-2 cell monolayer.

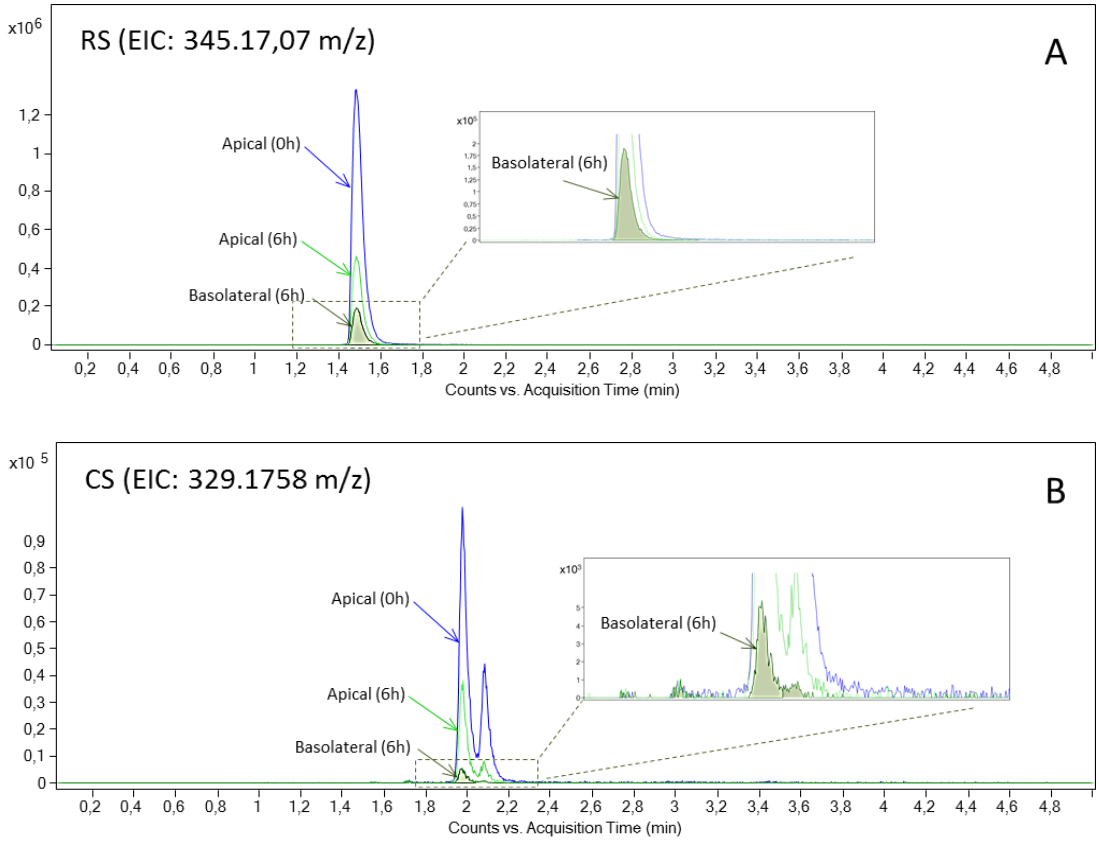

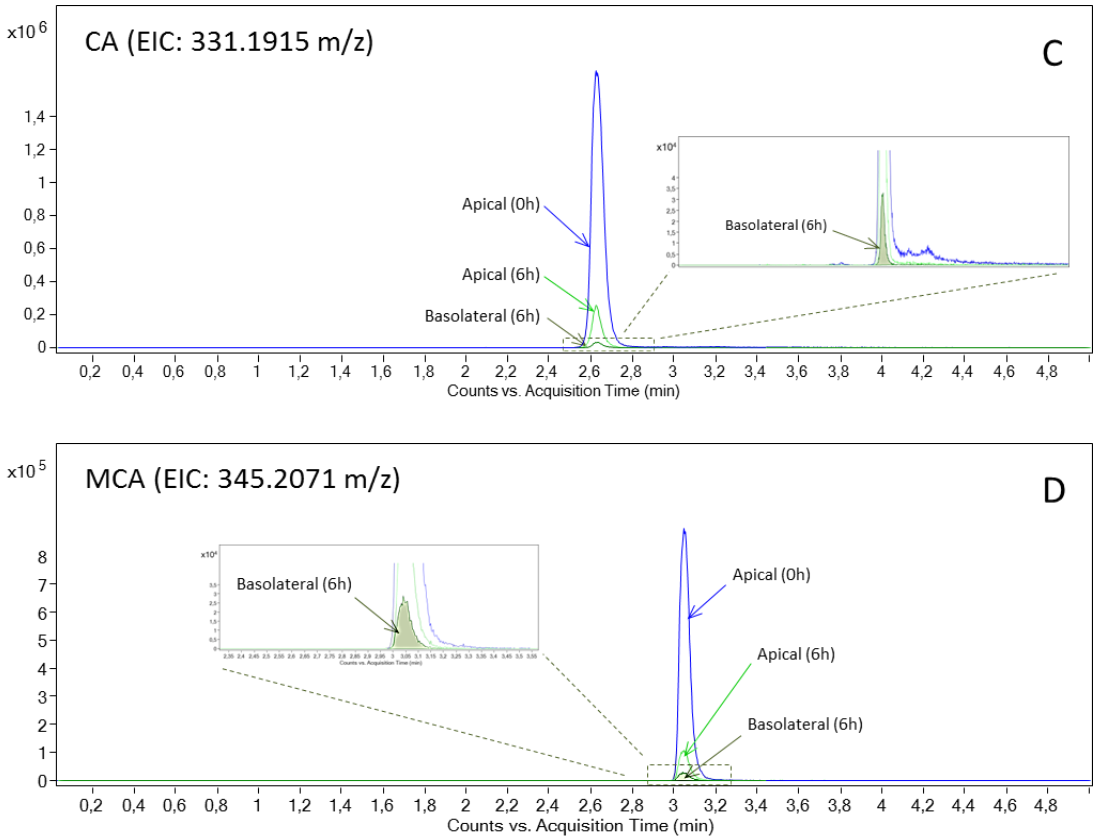

Figure 2.14. *Extracted Ion Chromatograms from standard compounds RS (A), CS (B), CA (C) and MCA (D), detected in the apical chamber at the beginning (blue line) and at the end (light green line) of the experiment, and detected in the basolateral chamber at the end of the experiment (dark green line).*

From UHPLC-TOF MS analyses of the apical and basolateral chambers before and after the experiment, P_{app} values were determined for each standard compound across Caco-2 cell monolayers and the summary of the permeability data is shown in **Table 2.9**.

Table 2.9. Permeability of CA, CS, RS and MCA as pure compounds during bidirectional transport study.

Compound	**P_{app} ($x10^{-6}$)**	
	AP-BL	**BL-AP**
CA	1.76 ± 0.20	1.64 ± 0.15
CS	8.75 ± 2.19	5.32 ± 0.32
RS	7.46 ± 0.79	9.24 ± 0.64
MCA	1.46 ± 0.16	3.67 ± 0.74

As it can be observed, $P_{app\ (BL\text{-}AP)}$ of the four compounds was greater than their $P_{app\ (AP\text{-}BL)}$.

2.2.4.2.3. Bi-directional transport of RE and GI-RE in Caco-2 monolayer

Transport across the Caco-2 cell monolayer of RS, CS, CA, and MCA in RE and GI-RE, was also evaluated.

For the permeability experiment with the rosemary extract, non-cytotoxic concentration of RE was placed in the donor chamber (apical or basolateral) and blank HBSS in the receiver compartment and incubated in presence of Caco-2 monolayer. Samples from the apical and basolateral compartments were collected at the beginning and at the end of incubation period and analyzed UHPLC-TOF MS. Then, Papp values were determined for RS, CS, CA and MCA, which are the main diterpenes found in the rosemary extract.

The following **Figure 2.15.** shows typical extracted ion chromatograms (EICs) from CA, CS, RS and MCA found in the RE in the AP-BL direction experiment.

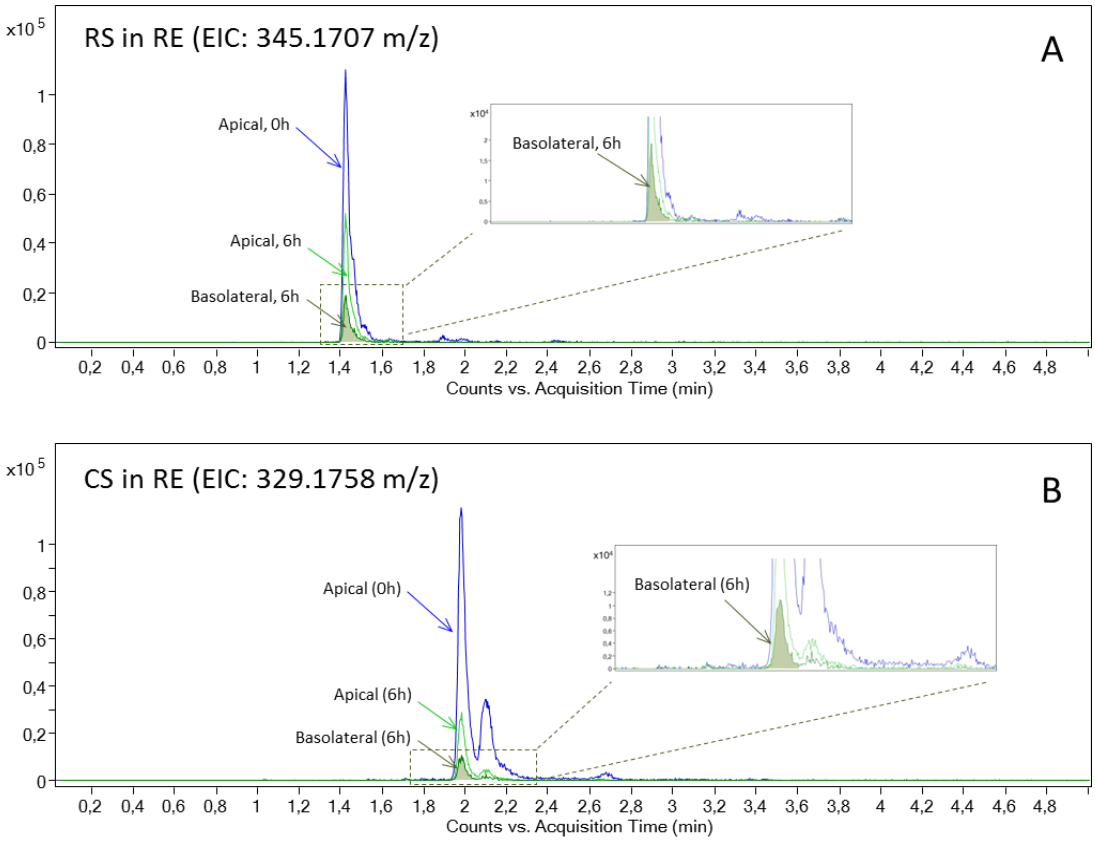

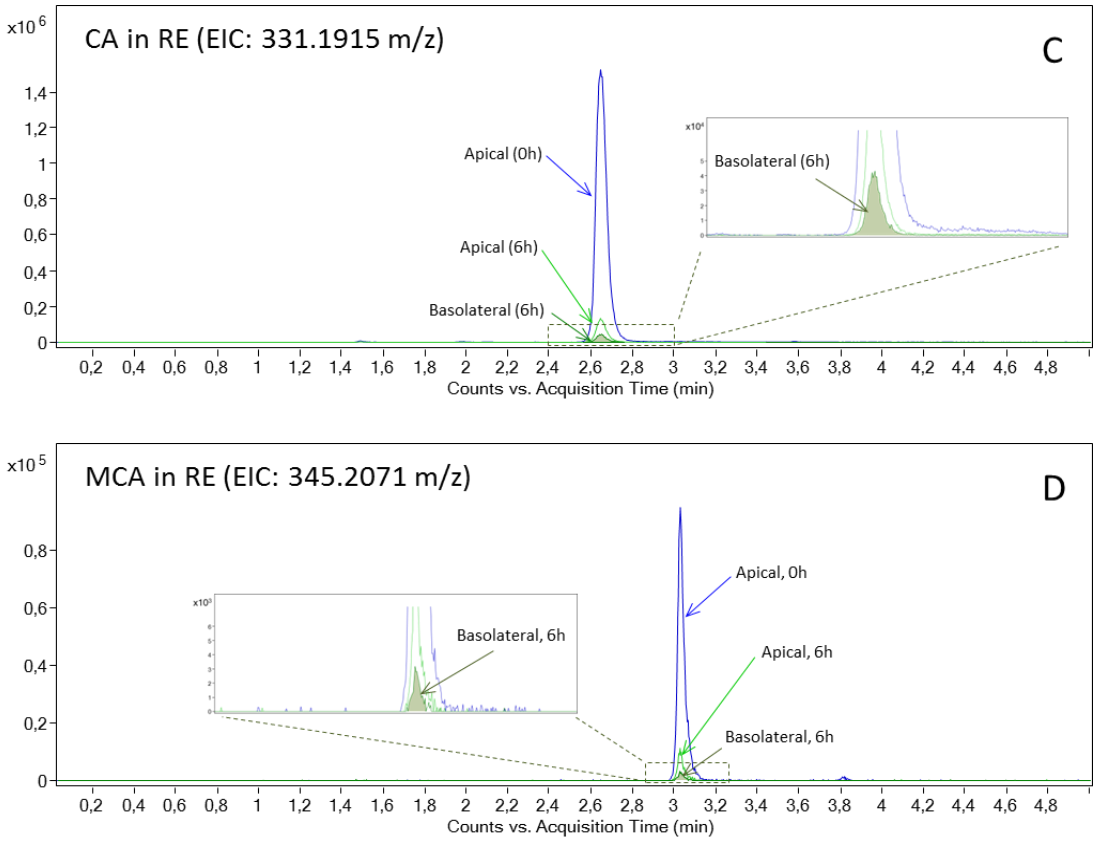

Figure 2.15. *Extracted Ion Chromatograms from standard compounds RS (A), CS (B), CA (C) and MCA (D) from RE, detected in the apical chamber at the beginning (blue line) and at the end (light green line) of the experiment, and detected in the basolateral chamber at the end of the experiment (dark green line).*

From UHPLC-TOF MS analyses of the apical and basolateral solutions before and after the transport experiment with RE, P_{app} values were determined for CA, CS, RS and MCA across Caco-2 cell monolayers and the summary of the permeability data is shown in **Table 2.10**.

Table 2.10. Permeability of CA, CS, RS and MCA in RE during bidirectional transport study.

Compound	**P_{app} ($x10^{-6}$)**	
	AP-BL	**BL-AP**
CA in RE	1.67 ± 0.06	2.41 ± 0.53
CS in RE	6.37 ± 0.91	6.61 ± 0.21
RS in RE	9.45 ± 0.18	9.50 ± 0.47
MCA in RE	1.99 ± 0.24	3.44 ± 0.88

As occurred in the transport of single compound across the Caco-2 cell monolayer, it was observed that the $P_{app\ (BL \rightarrow AP)}$ of the four compounds contained in the RE was also greater than their $P_{app\ (AP \rightarrow BL)}$.

For the permeability experiment with the gastrointestinal digestion product from the rosemary extract, a non-cytotoxic concentration of SPE-treated GI-RE (SPE/GI-RE) was placed in the donor chamber (apical or basolateral) and blank HBSS in the receiver compartment. After incubation in presence of Caco-2 monolayer for 6 h, solutions from donor and receiver chambers were collected and analyzed UHPLC-TOF MS. The following **Figure 2.16.** shows typical extracted ion chromatograms (EICs) from CA, CS, RS and MCA found in the SPE/GI-RE in the AP-BL direction experiment.

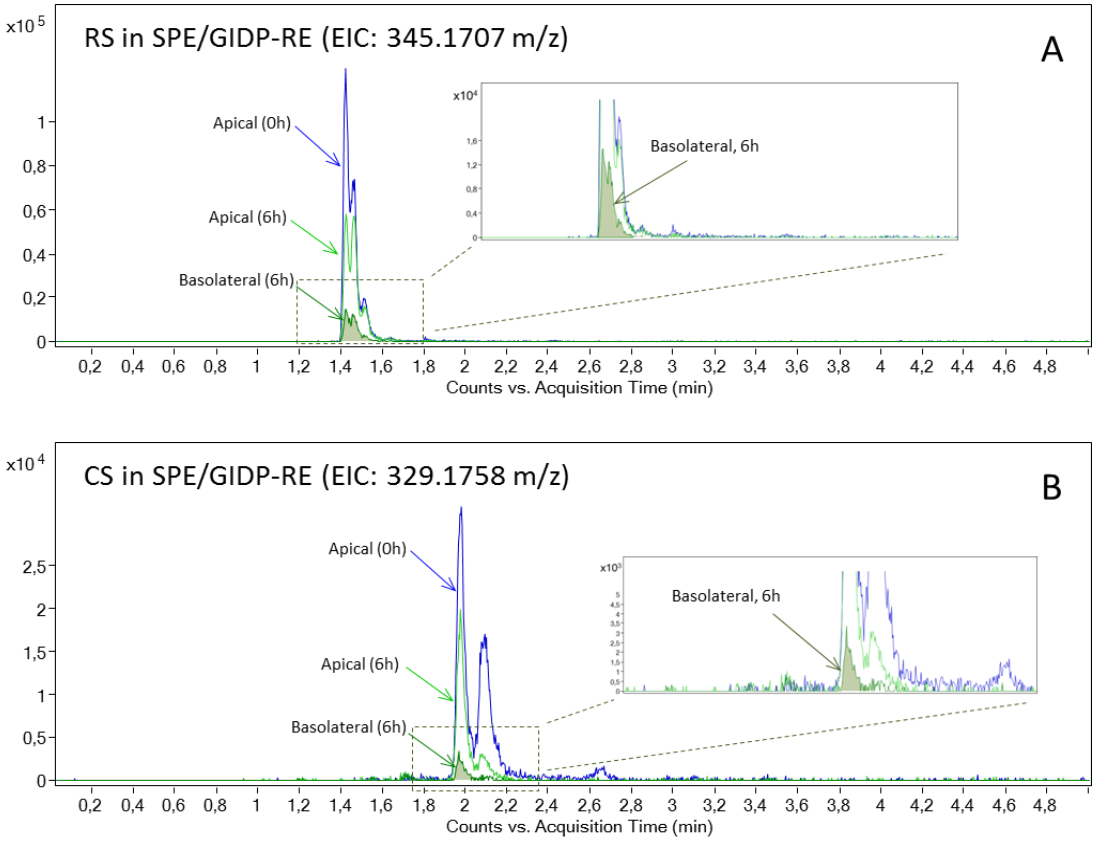

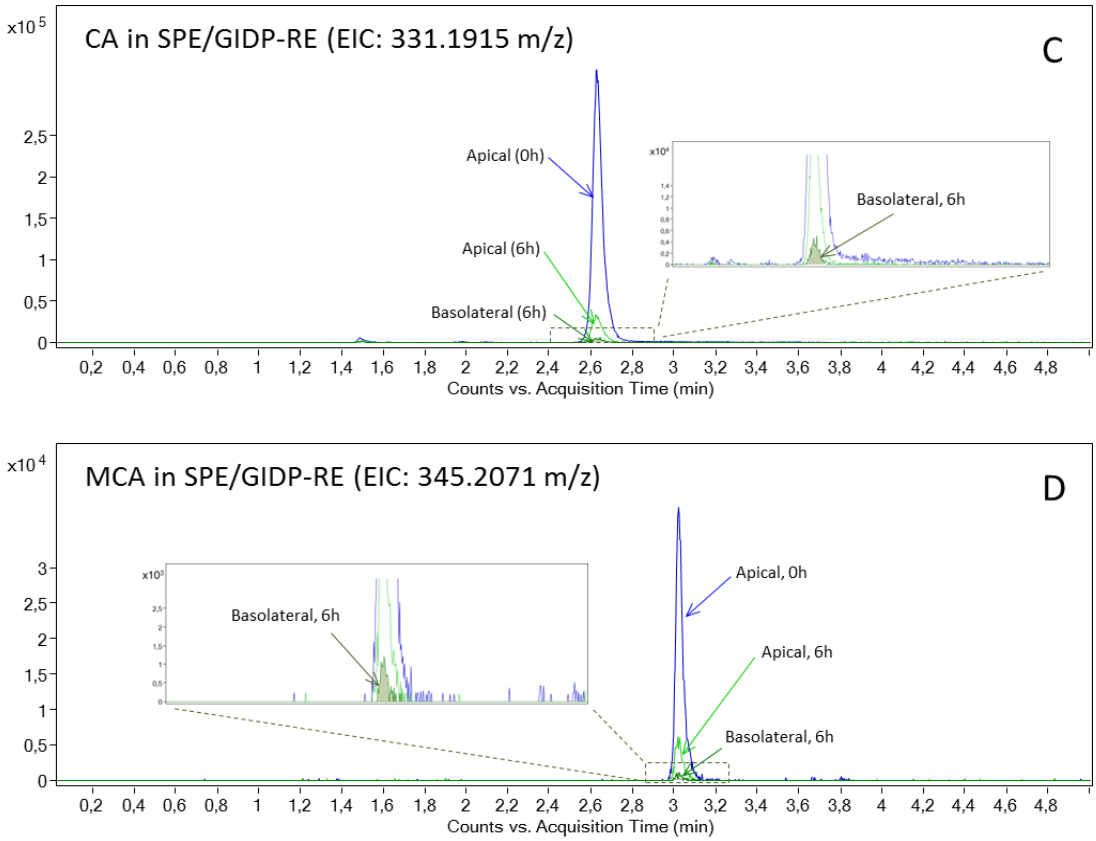

Figure 2.16. *Extracted Ion Chromatograms from standard compounds RS (A), CS (B), CA (C) and MCA (D) from RE, detected in the apical chamber at the beginning (blue line) and at the end (light green line) of the experiment, and detected in the basolateral chamber at the end of the experiment (dark green line).*

From UHPLC-TOF MS analyses of the apical and basolateral solutions before and after the transport experiment with SPE/GI-RE, P_{app} values were determined for CA, CS, RS and MCA across Caco-2 cell monolayers and the summary of the permeability data is shown in **Table 2.11**.

Table 2.11. Permeability of CA, CS, RS and MCA in SPE/GI-RE during bidirectional transport study.

Compound	**P_{app} ($x10^{-6}$)**	
	AP-BL	**BL-AP**
CA in SPE/GI-RE	0.91 ± 0.08	1.07 ± 0.15
CS in SPE/GI-RE	5.53 ± 0.27	18.89 ± 1.17
RS in SPE/GI-RE	8.94 ± 0.40	15.50 ± 0.48
MCA in SPE/GI-RE	1.67 ± 0.19	2.00 ± 0.21

Also, a non-cytotoxic concentration of U/GI-RE was assayed, and as we did for the previous experiments, U/GI-RE was placed in the donor chamber (apical or basolateral) and blank HBSS in the receiver compartment and incubated in presence of Caco-2 monolayer. Samples from the apical and basolateral compartments were collected at the beginning and at the end of incubation period and analyzed UHPLC-TOF MS. Unfortunately, at non cytotoxic concentration of U/GI-RE, main diterpenes could be detected in donor but not in the receiver chambers, and thus, P_{app} values could not be calculated.

After the calculation of P_{app} of CA, CS, RS and MCA, as individual compounds and in RE, we compared these values (**Figure 2.17.**).

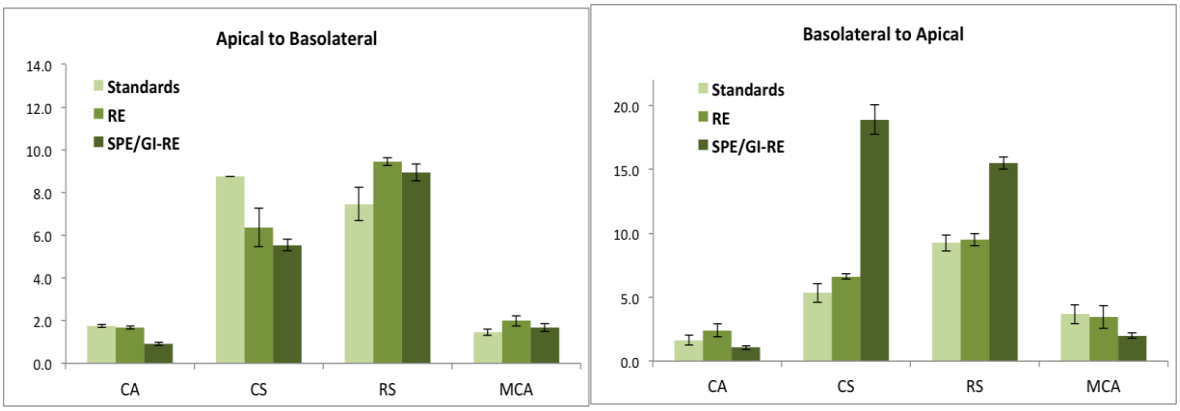

Figure 2.17. *Permeability of CA, CS, RS and MCA as individual test compounds (light green bars) and in the RE (dark green bars), during bidirectional transport study.*

Epithelial cells are polarized, meaning that they possess a distinct apical membrane facing the intestinal lumen and a basolateral membrane facing the sub-epithelial tissues, with different protein and lipid compositions, and thus different permeability properties [50]. The $P_{app\ (BL \rightarrow AP)}$ of the four diterpenes as single compounds but also contained in the RE and the SPE/GI-RE was greater than their $P_{app\ (AP \rightarrow BL)}$, revealing that rosemary diterpenes are more effectively absorbed across the basolateral membrane [51].

In general, higher values of P_{app} were observed for polyphenols in RE and SPE/GI-RE samples suggesting that plant matrix components and SPE procedure might alter the transport of the studied compounds. Moreover, in a complex extract there are interferences among the different compounds. Although the study of the absorption of the extract

resembles the *in vivo* processes in a better way, the study of pure compounds is better for the elucidation of the transport mechanism [52].

In agreement with the general permeability classification, in any case all the tested compounds presented low to medium permeability [36]. According to their P_{app} values, polyphenols could be ranked as following: RS>CS>MCA>CA. As it is known the degree of ionization of a drug is directly related to absorption and bioavailability. For CS and RS, pH (7.4) is lower than their pk_a (pk_a=9.19 for CS and pk_a=9.18 for RS). Hence, the major part of their molecules is protonated. Therefore, CS and RS are favored to diffuse across the lipid membrane of cells in comparison to CA (pk_a=4.29) and MCA (pk_a=4.46), which are mainly ionized [53].

2.2.4.2.4. Efflux of phenolic compounds from rosemary in Caco-2 monolayer

Efflux ratios (EfR) for CA, CS, RS and MCA were calculated according to **Equation 2.4.** given in Materials and Methods section (see **Section 2.1.7.4.**).

Table 2.12. Efflux ratios for CA, CS, RS and MCA as pure compounds and in RE and SPE/GI-RE during bidirectional transport study.

Compound	Efflux ratio		
	Standards	**RE**	**SPE/GI-RE**
CA	0.93 ± 0.02	1.43 ± 0.26	1.16 ± 0.07
CS	0.66 ± 0.20	1.06 ± 0.11	3.41 ± 0.04
RS	1.24 ± 0.05	1.01 ± 0.07	1.73 ± 0.02
MCA	2.59 ± 0.78	1.70 ± 0.23	1.20 ± 0.01

An efflux ratio of 1 was indicative of passive diffusion; values less than 0.5 and greater than 2 were regarded as being indicative of active influx (carrier-mediated transport) and active efflux (carrier-mediated efflux), respectively [25, 54]. Caco-2 cell line is derived from a human colorectal carcinoma and these cells strongly express P-gp transporter [55, 56]. P-gp is an ATP-dependent efflux transport protein, which act as first line of defense in the intestine facilitating the secretion of xenobiotic compounds from basolateral to apical chamber (*in vivo* from blood to lumen) reducing the net absorption of the compound [37].

Our results indicate that the intestinal absorption mechanism of rosemary phenolic compounds was mainly based on passive transcellular transport. However, EfR value for MCA as pure standard shows that MCA might be a substrate of P-gp, undergoing active efflux transport. Furthermore, MCA as a single compound was tested at higher concentration than the one contained in RE, since CA and CS are the most abundant polyphenols present in rosemary. Therefore, MCA might follow a concentration-dependent transport and approach saturation at this concentration, implying that MCA is poorly absorbed via intestine at high concentration [51, 57].

2.3. CONCLUSIONS

A significant loss of the main phenolic compounds in RE (CA, CS, RS, MCA) and the appearance of a new peak corresponding to CA-quinone, which is an intermediate in the degradation pathway of CA, were observed after GI digestion. In addition, GI- stability control sample was found highly toxic against Caco-2 cells, probably due to the presence of high concentration of biliary salts and digestive enzymes. Ultrafiltration and a SPE procedure were examined as purification strategies in order to eliminate those cytotoxic interfering compounds in GI-RE sample.

From the quantification of total phenols content, SPE/GI-RE presented to obtain the highest total phenol content. In terms of cytotoxicity, phenolic composition in SPE/GI-RE was more bioactive, followed by RE and U/GI-RE, respectively. Interestingly, UHPLC-TOF analysis revealed differences not only in total phenolic, but also in individual phenolic compound content between the two purified (SPE and ultrafiltrated) GI-RE samples. More specifically, higher concentration of the main rosemary diterpenes was detected in SPE/GI-RE sample. Also, two isomers of RS (epirosmanol and epiisorosmanol) could be detected.

According to the results of cytotoxicity tests, when Caco-2 cells were treated with pure phenolic standards (CA, CS, RS and MCA), rosemary diterpenes exerted a concentration-dependent cytotoxicity effect after 24 h of incubation of Caco-2 cells. RS exhibited the highest toxicity among them, while MCA showed the lowest.

On the other hand, the stability study at the donor compartment in absence of cells revealed that MCA was the more stable diterpene. CA was degraded mainly to CS and RS, while RD, RS-Q and traces of CA-Q were also observed. At the same time, RS was the main degradation product of CS, with RD and RS-Q detected as secondary degradation products. Finally, RS was degraded to RD and RS-Q.

In the presence of cell monolayer our data indicate the uptake of CA, RS and MCA from Caco-2 cells. Rosemary phenolic compounds are more effectively absorbed across basolateral membrane, since $P_{app\ (BL\rightarrow AP)}$ was found higher than $P_{app\ (AP\rightarrow BL)}$ when pure standards or diterpenes within the RE and SPE/GI-RE were studied. Our data also revealed that plant matrix components and SPE procedure affect the transport of diterpenes across the Caco-2 monolayer. All the compounds presented low to moderate P_{app} values. In addition, RS showed the highest P_{app} value, followed by CS, MCA and then CA. Finally, the calculated EfR values in this work indicate that the absorption mechanism of rosemary

diterpenes via intestine was mainly based on passive transcellular transport. Active efflux transport might be involved in MCA transport; however further experiments are needed to prove this.

CHAP.3 REFERENCES

1. Cui, L., Kim, M., O., Seo, J., H., Kim, I., S., Kim, N., Y., Lee, S., H., Park, J., Kim, J. and Lee H., S., Food Chem, 2012, **132**, 1775-1780.
2. Borras-Linares, I., Stojanovic, Z., Quirantes-Pine, R., Arraez-Roman, D., Svarc-Gajic, J., Fernandez-Gutierrez, A. and Segura-Carretero, A., Int. J. Mol. Sci., 2014, **15**, 20585-20606.
3. Perez-Fons L., Aranda, F., J., Guillen, J., Villalain, J. and Micol, V., Arch Biochem Biophys, 2006, **453**, 224-236.
4. Richheimer, S., L., Bernart, M., W., King, G., A., Kent, M., C. and Bailey, D., T., JAOCS, 1996, **73**, 507-514.
5. Bai, N., He, K., Roller, M., Lai, C.-S., Shao, X., Pan, M.-H. and Ho, C.-T., J. Agric. Food Chem., 2010, **58**, 5363-5367.
6. Rodriguez-Solana, R., Salgado, J., M., Dominguez, J., M. and Cortes-Dieguez, S., Phytochem. Anal., 2015, **26**, 61-71.
7. Arranz, E., Santoyo, S., Jaime, L., Fornari, T., Reglero, G., Guri, A., Corredig, M., Food Dig. Res Curr Opin, 2015, **6**, 30-37.
8. https://pubchem.ncbi.nlm.nih.gov/ (last visit October 2016)
9. Gonzalez-Vallinas, M., Gonzalez-Castejon, M., Rodriguez-Casado, A. and Ramirez de Molina, A., Nutr. Rev., 2013, **71**, 585-599.
10. Jacotet-Navarro, M., Rombaut, N., Fabiano-Tixier, A.-S., Danguien, M., Bily, A. and Chemat, F., Ultrason Sonochem, 2015, **27**, 102-109.
11. Birtic, S., Dussort, P., Pierre, F., X., Bily, A., C. and Roller, M., Phytochemistry, 2015, **115**, 9-19.
12. Bakirel, T., Bakirel, U., Keles, Ü., O., Ülgen, S., G. and Yardibi, H., J Ethnopharmacol, 2008, **116**, 64-73.
13. Johnson, J., J., Cancer Lett., 2011, **305**, 1-7.
14. Debersac, P., Vernevaut, M.-F., Amiot, M.-J., Suschetet, M., Siess, M.-H., Food Chem Toxicol., 2001, **39**, 109-117.
15. Tu, Z., Moss-Pierce, T., F., P. and Jiang, T., A., J. Agric. Food Chem., 2013, **61**, 2801-2810.
16. Slamenova, D., Kuboskova, K., Horvathova, E. and Robichova, S., Cancer Lett., 2012, **177**, 145-153.

17. Cheng, A.-C., Lee, M.-F., Tsai, M.-L., Lai, C.-S., Lee, J. H., Ho, C.-T., Pan, M.-H., Food Chem Toxicol., 2011, 49, 485-493.
18. Rivas, C.S., Marin, F.R., Santayo, S., Risco, M.R.G., Señorans, J. and Reglero G., J. Agric. Food Chem. 2010, **58**, 1144–1152.
19. Kong, F., and Singh, R.P., J Food Sci, 2010, **75**, 627-634.
20. Verhoeckx, K., Cotter, P., Expósito, I.L., Kleiveland, C., Mackie, T.A., Requena, T., Swiatecka, D. and Wichers, H., The Impact of Food Bio-Actives on Health: In Vitro and Ex Vivo Models, 1st ed., Cham, Switzerland, 2015, pp. 3-36.
21. Minekus, M., Alminger, M., Alvito, P., Ballance, S., Bohn, T., Bourlieu, C., Carriere, F., Boutrou, R., Corredig, M., Dupont, D., Dufour, C., Egger, L., Golding, M., Karakaya, S., Kirkhus, B., Le Feunteun, S., Lesmes, U., Macierzanka, A., Mackie, A., Marze, S., McClements, D. J., Menard, O., Recio, I., Santos, C. N., Singh, R. P., Vegarud, G. E., Wickham, M. S. J., Weitschies, W., and Brodkorb, A., Food Funct, 2014, **5,** 1113-1121.
22. Versantvoort, C.H.M., Oomen, A.G., Kamp, E.V., Rompelberg, C.J.M. and Sips, A.J.A.M., Food Chem Toxicol, 2005, **43**, 31–40.
23. Murota, K., and Terao, J., Arch. Biochem. Biophys., 2003, **417**, 12-17.
24. Yamashita, S., Furubayashi, T., Kataoka, M., Sakane, T., Sezaki, H., and Tokuda, H., Eur. J. Pharm. Sci., 2000, 10, 195-204.
25. http://www.cyprotex.com/admepk/in-vitro-permeability/caco-2-permeability (last visit November 2016)
26. Versantvoort, C., H., M., Ondrewater, R., C., A., Duizer, E., Van de Sandt, J., J., M., Gilde, A., J., and Groten, J., P., Environ. Toxicol. Pharmacol., 2002, **11**, 335-344.
27. Pontier, C., Pachot, J., Botham, R., Lenfant, B., and Arnaud, P., J. Pharm. Sci., 2001, **90**, 1608-1619.
28. Markowska, M., Oberle, R., Juzwin, S., Hsu, C.-P., Gryszkiewicz, M., and Steeter, A., J Pharmacol Toxicol Methods, 2001, **46**, 51-55.
29. Thanou, M., Verhoef, J., C., Marbach, P., and Junginger, H., E., J. Pharm. Sci., 2000, **89**, 951-957.
30. Antunes, F., Andrade, F., Araujo, F., Ferreira, D., and Sarmento, B., Eur. J. Pharm. Biopharm., 2013, **83**, 427-435.

31. Yan, Z., and Caldwell, G.C., Methods in Pharmacology and Toxicology Optimization in Drug Discovery: In vivo Methods, 1st ed., Humana Press Inc., Totowa, NJ, 2004, pp. 19-33.
32. Artursson, P., Palm, K., and Luthman, K., Adv. Drug Deliv. Rev., 2001, **46**, 27-43.
33. Daugherty, A., L., and Mrsny, J., PSTT, 1999, **2**, 144-151.
34. Sugano, K., Kansy, M., Artursson, P., Avdeef, A., Bandels, S., Di, L., Ecker, G., F., Faller, B., Fischer, H., Gerebtzoff, G., Lennernaes, H., and Senner, F., Nat. Rev. Drug Discov., 2010, **9**, 597-614.
35. Varma, M., V., S., Sateesh, K., and Panchagnula, R., Mol. Pharm., 2004, **2**, 12-21.
36. http://www.cerep.fr/cerep/users/pages/Downloads/Documents/Marketing/Pharmacology%20&%20ADME/Application%20notes/2013/In%20vitro%20drug%20absorption.pdf (last visit November 2016).
37. Chan, L., M., S., Lowes, S., and Hirst, H., Eur. J. Pharm. Sci. 2004, **21**, 25-51.
38. Herrero, M., Plaza, M., Cifuentes, A., and Ibáñez, E., J. Chromatogr. A, 2010, **1217** (16), 2512-2520.
39. Koşar, M., Dorman, H., J., D., and Hiltunen, R., Food Chem., 2005, **91**, 525-533.
40. Yee, S., Pharm Res., 1997, **14** (6), 763-766.
41. Zhang, Y., Smuts, J., P., Dodbiba, E., Rangarajan, R., Lang, J., C., and Armstrong, D., W., J Agric Food Chem, 2012, **60**, 9305-9314.
42. Charlton, A., Baxter, N., J., Khan, M., L., Moir, A., J., G., Haslam, E., Davies, A., P., and Williamson, M., P., J Agric Food Chem, 2002, **50**, 1593-1601.
43. Valdés, A., García-Cañas, V., Simó, C., Ibáñez, C., Micol, V., Ferragut, J. A., and Cifuentes, A., Anal. Chem. 2014, **86**, 9807-9815.
44. Vaquero, M., R., Villalba, R., G., Larrosa, M., Yañez-Gascon, M., J., Fromentin, E., Flanagan, J., Roller, M., Tomas-Barberan, F., A., Espin, J., C., and García-Conesa, M., T., Mol. Nutr. Food Res., 2013, **57**, 1834-1846.
45. Vogelpoel, H., Welink, J., Amidon, G., L., Junginger, H., E., Midha, K., K., Möller, H., Olling, M., Shah, V., P., and Barends, D., M., J. Pharm. Sci., 2004, **93** (8), 1945-1956.
46. Teksin, Z., S., Seo, P., R., and Polli, J., E., AAPS J., 2010, **12** (2), 238-241.
47. Parr, A., Hidalgo, I., J., Bode, C., Brown, W., Yazdanian, M., Gonzalez, M., A., Sagawa, K., Miler, K., Jiang, W., and Stippler, E., S., Pharm. Res., 2016, **33**, 167-176.

48. Vogelpoel, H., Welink, J., Amidon, G., L., Junginger., H., E., Midha, K., K., Moller, H., Olling, M., Shah, V., P., and Barends, D., M., J. Pharm. Sci., 2004, **93** (8), 1945-1956.
49. Jipa, S., Zaharescu, T., Kappel, W., Dumitrescu, C., Maris, M., Mantsch, A., amd Lungulescu, M., J. Optoelectron. Adv. M., 2008, **10**, 669-673.
50. Simons, K., van Meer, G., Biochemistry, **27** (17), 1988, 6197-6202.
51. Lu, Y., Zhang, J., Wan, X., Long, M., Li, D., Lei, P., and Zhang, Z., Food Chem., 2011, **125** (2), 277-281.
52. Borrás-Linares, I., Herranz-López, M., Barrajón-Catalán, E., Arráez-Román, D., González-Álvarez, I., Bermejo, M., Gutiérrez, A., F., Micol, V., and Segura-Carretero, A., Int. J. Mol. Sci., 2015, **16**, 18396-18411.
53. https://chemicalize.com (last visit November 2016).
54. Kratz, J., M., Teixeira, M., R., Koester, L.S., and Simoes, C., M., O., Braz. J. Med. Biol. Res., 2011, **44**, 531-537.
55. Antunes, F., Andrade, F., Araujo, F., Ferreira, D., and Sarmento, B., Eur. J. Pharm. Biopharm., 2013, **83**, 427-435.
56. Gutmann, H., Fricker, G., Torok, M., Michael, S., Beglinger, C., and Drewe, J., Pharm. Res., 1998, **16** (3), 402-407.
57. Chen, L., Lu, X., Liang, X., Hong, D., Guan, Z., Guan, Y., and Zhu, W., Acta Pharm. Sin. B, 2016, **6** (2), 125-131.

ANNEXES

ANNEX A: CELL VIABILITY TESTING

A.1. Trypan blue Assay

Trypan blue (TB) (tetrasodium;(3Z)-5-amino-3-[[4-[4-[(2Z)-2-(8-amino-1-oxo-3,6 disulfonatonaphthalen-2-ylidene)hydrazinyl]-3-methylphenyl]-2methylphenyl]hydrazinylidene]-4-oxonaphthalene-2,7-disulfonate, $C_{34}H_{24}N_6Na_4O_{14}S_4$) is a blue acid stain that contains two azo chromophores [1, 2]. It's a large, hydrophilic tetrasulfonated molecule, which is used as a vital dye. It is commonly used for cell counting (alive and dead) with hemocytometer under microscope, especially during routine subculturing [2, 3].

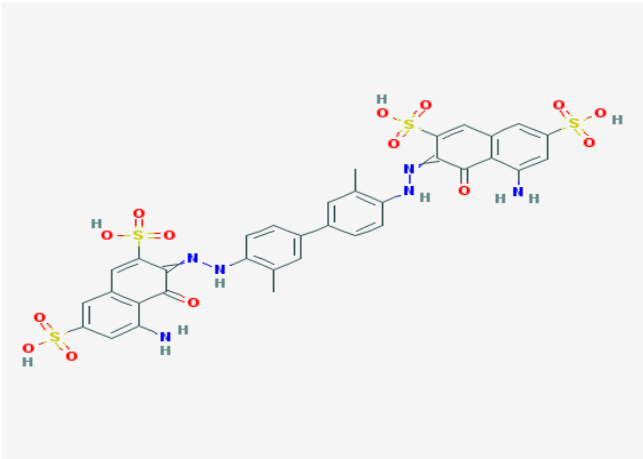

Figure A.1. *The structure of Trypan Blue molecule [1].*

Hence, Trypan blue (TB) is used very frequently in a staining method, which is based on the concept that viable cells do not take up certain dyes (like TB), whereas dead cells are permeable to them and take them up [4]. Thus, dead cells stain blue, while alive cells exclude TB. For that reason this type of method is also known as dye exclusion method [3].

More specifically, the cells membrane is impermeable to TB, which is a ~960 Daltons molecule. Thus, TB only enters cells with non-intact membranes. It traverses the cell membrane and as it enters into the cell, TB binds to intracellular proteins rendering them a dark blue color. Therefore, this method permits the enumeration of viable (unstained) and non viable (blue) cells in a given cells population and also the determination of cells viability [3, 5]. Furthermore, it is worth noting that the method cannot distinguish between necrotic and apoptotic cells [6].

TB staining method is a simple, quick, cheap and accurate method, where only a small

fraction of the total initial cells is used. Also, this method permits the counting of viable cells as well as dead cells simultaneously but also the calculation of cell viability, namely the percentage of cells in a cell suspension that is viable. However, special precaution must be taken (use of gloves and hood) during the handling of TB, since there are references about its carcinogenicity [3, 5].

A.2. MTT Assay

MTT-assay is a colorimetric enzyme-based assay widely used in the determination of cells viability or cytotoxicity tests. Its success is based on the fact that it is easy to use, it constitutes a safe and cheap method with high reproducibility, it can be used in almost all eukaryotic cell lines including adherent and non-adherent cells and certain tissues, and there is no need to transfer the cells, since the entire assay is performed on a well-plate. The MTT assay measures the cell proliferation rate and conversely, when metabolic events lead to apoptosis or necrosis, the reduction in cell viability [7, 8].

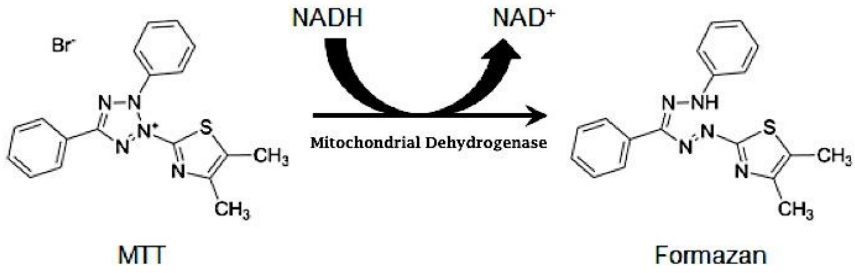

Figure A.2. *The chemical reaction of the transformation of the yellow MTT to the purple Formazan through the action of a mitochondrial dehydrogenase, when MTT is added to viable cells [9].*

The major principle of the assay is based on the reduction of yellow MTT [3- (4,5-dimethyl-2-thiazolyl)-2,5-diphenyl-2H-tetrazolium bromide] by metabolically active cells to a purple Formazan, involving the action of mitochondrial dehydrogenase enzymes. The amount of the formed Formazan can be quantified by measuring Absorbance.

The exact mechanism of MTT reduction into Formazan is not yet fully clarified, but it seems that involves reaction with NADH, NADPH or similar reducing molecules that function as electrons carriers to MTT. MTT tetrazolium is positively charged, so it easily penetrates viable eukaryotic cells. Only viable cells with active metabolism are able to

convert MTT into Formazan. When a cell dies, it rapidly loses its ability for this conversion, since it cannot produce dehydrogenases any more. Therefore, the amount of Formazan (measured as Absorbance) is proportional to the number of living cells [9].

Cells can be placed in the wells of a plate and then be treated with compounds or agents that affect proliferation. Cells are then detected with the addition of the proliferation reagent MTT prepared in a physiologically balanced solution, such as Phosphate Buffer Saline (PBS). MTT solution is added to cells usually at a final concentration from 0.2 to 0.5 mg/mL and then incubated for 1 to 4 hours. The conversion of MTT into Formazan is time dependent. Longer incubation time leads to more intense color, thus to increased sensitivity, and shorter incubation time to a softer color. However, there is a limit regarding the incubation time due to the cytotoxic nature of the detection reagents, which uses energy from the cell (reducing equivalents such as NADH and NADPH) in order to produce signal. In addition, due to MTT cytotoxicity cells that are used in MTT assay can be used in another assay, since it has been reported that Formazan crystals harm cells by puncturing membranes during exocytosis [9].

MTT-Formazan, which is formed during the incubation, is insoluble in water and forms purple needle-shaped crystals in cells. Hence, prior to absorbance measuring an organic solvent, usually dimethyl sulfoxide, is needed in order to solubilize the crystals and obtain an homogenous colored solution, the absorbance of which can be measured by spectrophotometric means such as a microplate reader [7, 10].

Figure A.3. *The different nuances obtained after the MTT assay in a 96-well plate. More intense color signifies a higher number of viable cells [11].*

In the absence of cells, MTT presents low background absorbance values. During the assay, triplicates should be used for each condition. The assay must also includes blank

wells (containing only medium), untreated control cells and cells treated with the examined substance. The absorbance value in each well that contains treated cells is compared to the absorbance of control cells. Every absorbance lower than that of the control cells indicates a reduction in cell viability due to a toxic compound or suboptimal culture conditions. Conversely, a higher absorbance value shows an increase in cells proliferation [10]. Finally, in some cases a shift from proliferation to quiescence can be observed and shows cytostatic activity. The amount of the generated signal is dependent on various parameters, such as the concentration of MTT, the time of incubation, the solubilization organic solvent, the number of viable cells and their metabolic activity. Furthermore, it must be noted that MTT is sensitive to light and should be kept in dark and at 4 ^{o}C. However, before its use MTT should be warmed at 37 ^{o}C [8, 9].

ANNEX B: VERIFICATION OF CELL MONOLAYER INTEGRITY

Integrity of a confluent and polarized monolayer can be verified in different ways. The most reliable methods between them are by measuring transepithelial electrical resistance (TEER), by measuring the passage of the fluorescent dye Lucifer Yellow or the permeability of reference compounds, such as atenolol (paracellularly transported) and propranolol (passive transcellularly transported) [12, 13].

TEER values are strong indicators of the integrity of the cellular barriers before they are evaluated for transport of drugs or other compounds. TEER represents the tightness of the cell-junction structure, and the paracellular permeability increases with decreasing TEER [14].

Lucifer Yellow (6-Amino-2,3-dihydro-1,3-dioxo-2-hydrazinocarbonylamino-1H-benz[d,e]isoquinoline-5,8-disulfonic acid dilithium salt, $C_{13}H_9Li_2N_5O_9S_2$) is a fluorescent dye, which can be easily used as a detectable paracellular marker [15,16]. Being a small hydrophilic molecule, Lucifer Yellow is incapable to cross trancellularly the monolayer, since it has a low affinity to the lipid cellular bilayer. Therefore, Lucifer yellow crosses the monolayer passively through the paracellular route. However, after 21 days of cultivation, Caco-2 cells form a confluent and polarized cell monolayer with tight junctions, where none or minimal paracellular flux is observed [17]. Thus, Lucifer Yellow can be used as a colorant marker in order to validate the integrity of Caco-2 monolayer by monitoring its permeation. The apical side of the monolayer is exposed to a concentration of Lucifer Yellow. High degree of Lucifer Yellow passage and its presence in the basolateral compartment indicate poor integrity and compromise of the monolayer [18]. The control can be done on separate wells or in parallel with the compound tested in the transport experiment. This control can be particularly useful during the studies of transepithelial transport of a test compound in order to determine the highest concentration of compound that can be tested without disturbing the uniformity of the cell-monolayer. Instead of Lucifer Yellow, other paracellular markers can also be used, with [^{14}C] mannitol being the most famous among them. However, Lucifer yellow outweighs [^{14}C] mannitol by being a non-radioactive alternative [17].

REFERENCES OF ANNEXES

1. https://pubchem.ncbi.nlm.nih.gov/ (last visit October 2016)
2. http://www.sigmaaldrich.com/catalog/product/aldrich/302643?lang=en&region=GR (last visit October 2016)
3. https://www.thermofisher.com/order/catalog/product/15250061 (last visit October 2016)
4. https://www.researchgate.net/file.PostFileLoader.html?id=54f44c67d2fd64f57e8b4651&assetKey=AS%3A273719526658055%401442271228688 (last visit October 2016)
5. http://www.nexcelom.com/Applications/measure-cell-viability-using-trypan-blue-or-AOPI.php (last visit October 2016)
6. http://groups.molbiosci.northwestern.edu/morimoto/research/Protocols/II.%20Eukaryotes/A.%20Cell%20Culture/3d.%20Trypan%20Blue%20Staining.pdf (last visit November 2016)
7. https://www.dojindo.com/Protocol/Cell_Proliferation_Protocol_Colorimetric.pdf (last visit October 2016)
8. http://www.cellbiolabs.com/sites/default/files/CBA-252-mtt-cell-proliferation-assay.pdf (last visit September 2016)
9. Sittampalam, G.S., Coussens, N.P., Nelson, H., Arkin, M., Auld, D., Austin, C., Bejcek, B., Clicksman, M., Inglese, J., Iversen, P.W., Li, Z., McGee, J., McManus, O., Minor, L., Napper, A., Peltier, J., M., Riss, T., Trask, O.J., and Weidner, J., Assay Guidance Manual, 1st ed., Eli Lilly & Company and the National Center for Advancing Translational Sciences, Bethesda, MD, 2004, pp. 262-292.
10. https://www.atcc.org/~/media/DA5285A1F52C414E864C966FD78C9A79.ashx (last visit October 2016)
11. http://www.bergmandiag.no/file/nedlast/applicationguideformultimodereaders397823v1.pdf (last visit October 2016)
12. Verhoeckx, K., Cotter, P., Expósito, I.L., Kleiveland, C., Mackie, T.A., Requena, T., Swiatecka, D. and Wichers, H., The Impact of Food Bio-Actives on Gut Health: In Vitro and Ex Vivo Models, 1st ed., Cham, Switzerland, 2015, pp. 95-102.
13. Srinivasan, B., Kolli, A., R., Esch, M., B., Abaci, H., E., Shuler, M., L., and Hickman, J., J., J. Lab. Autom., 2015, **20** (2), 107-126.

14. Versantvoort, C., H., M., Ondrewater, R., C., A., Duizer, E., Van de Sandt, J., J., M., Gilde, A., J., and Groten, J., P., Environ. Toxicol. Pharmacol., 2002, **11**, 335-344.
15. https://pubchem.ncbi.nlm.nih.gov/compound/20835957#section=3D-Conformer (last visit October 2016)
16. Hubatsch, I., Ragnarsson, E., G., E., and Artursson, P., Nat. Protoc., 2007, 2 (9), 2111-2119.
17. Minekus, M., Alminger, M., Alvito, P., Ballance, S., Bohn, T., Bourlieu, C., Carriere, F., Boutrou, R., Corredig, M., Dupont, D., Dufour, C., Egger, L., Golding, M., Karakaya, S., Kirkhus, B., Le Feunteun, S., Lesmes, U., Macierzanka, A., Mackie, A., Marze, S., McClements, D. J., Menard, O., Recio, I., Santos, C. N., Singh, R. P., Vegarud, G. E., Wickham, M. S. J., Weitschies, W., and Brodkorb, A., Food Funct, 2014, 5, 1113-1121.
18. http://www.brunswicklabs.com/pharmaceutics/adme/tox/caco-2-permeability-screening (last visit September 2016)